

**Hanford Tank Farms Vadose Zone**

**Seventh Recalibration of Spectral Gamma-Ray  
Logging Systems Used for Baseline Characterization  
Measurements in the Hanford Tank Farms**

**C.J. Koizumi**

**February 2000**

Prepared for  
U.S. Department of Energy  
Albuquerque Operations Office  
Grand Junction Office  
Grand Junction, Colorado

Prepared by  
MACTEC-ERS  
Grand Junction Office  
Grand Junction, Colorado

# Contents

	Page
<b>1.0 Overview and Summary of Results</b> .....	1
1.1 Overview .....	1
1.2 Calibration Function .....	3
1.3 Revised Field Verification Acceptance Criteria .....	5
1.4 Revised Corrections for Casing and Water-Filled Boreholes .....	7
<b>2.0 Revised Calibration Functions</b> .....	10
2.1 Calibration Standards .....	10
2.2 Data Acquisition .....	11
2.3 Data Analysis .....	11
<b>3.0 Linearity Test Results</b> .....	18
<b>4.0 Comparison of Seventh Recalibration with Previous Recalibrations</b> .....	23
<b>5.0 New Field Verification Criteria</b> .....	28
<b>6.0 Acknowledgments</b> .....	31
<b>7.0 References</b> .....	32
<b>Appendix A. Updated General Corrections for Borehole Casing</b> .....	A-2
<b>A1.1 Background</b> .....	A-2
<b>A1.2 Corrections Reformulated to Reduce Uncertainties</b> .....	A-3
<b>A1.2.1 Linear Interpolation for <math>F</math>, <math>G</math>, and <math>H</math></b> .....	A-3
<b>A1.2.2 Curve Fitting for <math>A_c</math> and <math>B_c</math></b> .....	A-4
<b>A1.3 The Recommended Method: Linear Interpolation for <math>A_c</math> and <math>B_c</math></b> ..	A-8
<b>A1.4 Summary</b> .....	A-11
<b>Appendix B. Updated General Corrections for Water-Filled Boreholes</b> .....	B-2
<b>B1.1 Background</b> .....	B-2
<b>B1.2 Gamma 2A Water Corrections</b> .....	B-3
<b>B1.3 Reformulated Water Corrections</b> .....	B-4
<b>B1.4 Summary</b> .....	B-7

# Contents (continued)

Page

## Figures

Figure 2-1. Calibration Data and Calibration Function for Gamma 2A Plotted in Relation to Gamma-Ray Energy .....	16
2-2. Calibration Data and Calibration Function for Gamma 2B Plotted in Relation to Gamma-Ray Energy .....	17
3-1. Gamma 2A Linearity Demonstration for 352.0-keV Gamma-Ray Data .....	19
3-2. Gamma 2A Linearity Demonstration for 1120.3-keV Gamma-Ray Data .....	20
3-3. Gamma 2A Linearity Demonstration for 2204.1-keV Gamma-Ray Data .....	20
3-4. Gamma 2B Linearity Demonstration for 295.2-keV Gamma-Ray Data .....	21
3-5. Gamma 2B Linearity Demonstration for 609.3-keV Gamma-Ray Data .....	21
3-6. Gamma 2B Linearity Demonstration for 1764.5-keV Gamma-Ray Data .....	22
4-1. Variation of the 1460.8-keV Gamma 2A Calibration Function with Time .....	24
4-2. <sup>40</sup> K Concentrations Calculated Using a Fixed Peak Intensity ( $12.23 \pm 0.70$ counts per second, the average intensity from the K Model measurements for the base calibration) and the $I(E)$ Values for the Various Calibrations .....	27

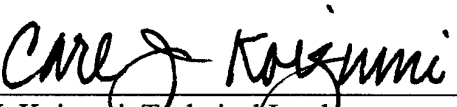
## Tables

Table 1-1. The Four Logging Systems .....	1
1-2. Constants for the Calibration Function .....	5
1-3. Field Verification Acceptance Criteria for Gamma 2A .....	6
1-4. Field Verification Acceptance Criteria for Gamma 2B .....	6
1-5. Casing Correction Parameters for Gamma 1A .....	8
1-6. Casing Correction Parameters for Gamma 2A .....	8
1-7. Gamma 2A Water Correction Parameter Values for the Most Common Borehole Diameters at Hanford .....	9
2-1. Calibration Standards and Their Source Concentrations .....	10
2-2. Reference Standards for Calibration Standard Source Concentrations .....	10
2-3. Calibration Model Source Intensities .....	13
2-4. Calibration Peak Intensities Recorded by Gamma 2A .....	14
2-5. Calibration Peak Intensities Recorded by Gamma 2B .....	15
3-1. Factors for the Dead Time Correction .....	18
4-1. Calibration Constants and Sample $I(E)$ Values for Gamma 2A and Gamma 2B ...	23
4-2. Illustrations of Logging System Efficiency Drifts .....	26
5-1. Outcomes of Field Verification Measurements .....	28
5-2. Outcomes of Field Verification Measurements Involving Follow-Up Spectra ....	29
5-3. Field Verification Acceptance Criteria for Gamma 1A .....	30
5-4. Field Verification Acceptance Criteria for Gamma 1B .....	30

## Hanford Tank Farms Vadose Zone

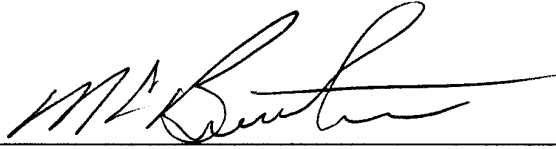
### Seventh Recalibration of Spectral Gamma-Ray Logging Systems Used for Baseline Characterization Measurements in the Hanford Tank Farms

Prepared by:

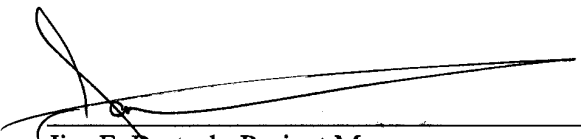
  
\_\_\_\_\_  
Carl J. Koizumi, Technical Lead  
MACTEC-ERS, Grand Junction Office

2/20/2000  
Date

Approved by:

  
\_\_\_\_\_  
Michael Butherus, Task Order Manager  
MACTEC-ERS, Grand Junction Office

2/28/00  
Date

  
\_\_\_\_\_  
Jim F. Bertsch, Project Manager  
MACTEC-ERS, Hanford Office

2/24/00  
Date

# 1.0 Overview and Summary of Results

## 1.1 Overview

The U.S. Department of Energy (DOE) Richland Operations Office (DOE-RL) enlisted the DOE Grand Junction Office (DOE-GJO) to develop a baseline characterization of the gamma-ray-emitting radionuclides that are constituents of the radioactive wastes that exist in the vadose zone sediments beneath and around the single-shell tanks (SSTs) at the Hanford Site. The baseline data are acquired by logging existing monitoring boreholes with high-resolution passive spectral gamma-ray logging systems (SGLSs). Analyses of the recorded spectra yield the pulse heights and intensities of the full energy spectral peaks (peaks). From the pulse heights, the gamma-ray energies are determined, and these energies are the basis for unambiguous identifications of the gamma-ray source nuclides. The peak intensities are used to calculate the concentrations of the source nuclides in the media surrounding the boreholes. These concentration calculations employ various corrections and the logging system calibration functions.

The acquisition of baseline characterization data began in 1995 with the deployment of two SGLSs, each consisting of a surface support system (vehicle, logging cable control system, data acquisition system electronics) and a sonde. In 1997 a third sonde was acquired. In routine operations, the original sondes are never exchanged between logging systems, but the third sonde is used as a backup component to either logging system. Thus, the two surface support systems and three sondes can be utilized in the four configurations displayed in Table 1-1.

*Table 1-1. The Four Logging Systems*

Surface Support System	Sonde	Logging System Name
Gamma 1 DOE Vehicle Number (HO68B3572)	original detector serial number (34TP20893A)	Gamma 1 or Gamma 1A
	backup detector serial number (36TP21095A)	Gamma 1B
Gamma 2 DOE Vehicle Number (HO68B3574)	original detector serial number (34TP11019B)	Gamma 2 or Gamma 2A
	backup detector serial number (36TP21095A)	Gamma 2B

Periodic recalibration of the SGLSs, as prescribed by the project document *Vadose Zone Monitoring Project at the Hanford Tank Farms, Spectral Gamma-Ray Borehole Geophysical Logging Characterization and Baseline Monitoring Plan for the Hanford Single-Shell Tanks* (DOE 1995a), ensures that the radionuclide concentrations derived from the log data are defensibly linked to DOE calibration standards. The (original) logging systems were calibrated at the beginning of the

characterization project. Those initial, or base, calibrations utilized the borehole gamma-ray calibration standards at DOE-GJO, and the measurements and results are documented in DOE (1995b). Subsequent recalibrations utilized the calibration standards at the Hanford borehole logging calibration center and were performed biannually. The first, second, third, fourth, and fifth biannual recalibrations are described in DOE (1996a), DOE (1996b), DOE (1997), DOE (1998a), and DOE (1998b), respectively.

Following the acquisition of data for the fifth biannual recalibrations in October 1997, MACTEC-ERS technical staff members evaluated the calibration and field verification data collected over the duration of the project, and determined that the stability of each logging system over time justified a change in the recalibration schedule from biannual to annual. Thus, the data for the sixth recalibration (DOE 1999) were acquired in the fall of 1998, and the data for the seventh recalibration were collected in the fall of 1999.

In 1999, logging with the Gamma 1A and Gamma 1B systems was curtailed to support logging with a new high-rate system. The Gamma 1 surface support system (logging truck and electronics) was eventually assigned full time to logging with the new system, and the down-hole components of the high-rate system were mounted in the Gamma 1A sonde housing. Because the Gamma 1A and Gamma 1B systems have not participated in SGLS logging since early 1999, these systems were not recalibrated in 1999. Only Gamma 2A and Gamma 2B were recalibrated for the seventh recalibration in 1999.

For the seventh recalibration, data were collected with Gamma 2A and Gamma 2B to accomplish the following:

- C The factors in the general calibration functions for natural and man-made gamma-ray sources were revised. For Gamma 2B the changes in the calibration function resulting from these revisions were minor and this logging system continued to exhibit the stability that was consistently observed during the previous recalibrations. The calibration function values for Gamma 2A were, at typical gamma-ray energies, about 3 percent higher than values for the sixth recalibration function, and about 12 percent higher than values for the fifth recalibration function. Because the efficiency and calibration function are inversely related, these results imply that the efficiency of Gamma 2A experienced a decrease of about 8 percent between the fifth and sixth recalibrations, and that after the sixth recalibration the efficiency continued to drift downward, but at a slower rate.
- C Linearity of logging system response in relation to source intensity was reconfirmed for both logging systems over a range of source intensities exceeding the range spanned by the sources in the calibration standards. These linearity demonstrations validate the system dead time corrections.
- C During logging operations, the performance of each logging system is frequently checked by recording spectra with a potassium-uranium-thorium source (Amersham *KUTh Field Verifier* [Amersham part number 188074]), then confirming that the intensities and full widths at half

maxima (FWHM) of selected spectral peaks fall within acceptable ranges. These parameter ranges, or field verification acceptance criteria, are reviewed and revised at each recalibration.

- C Corrections for casing and water-filled boreholes have been re-formulated. Casing corrections were first developed from base calibration measurements involving five discrete casing thicknesses (DOE 1995b). Sections of test casing that were available for measurements were used, but their thicknesses did not match the thicknesses of the casings installed in the Hanford boreholes. Similarly, the base calibration measurements for water-filled borehole corrections utilized the test holes in the DOE-GJO KW Model (Leino et al. 1994), but the diameters of those holes did not coincide with any of the borehole diameters at Hanford. Attempts to determine corrections for Hanford casing thicknesses and borehole diameters by curve fitting produced accurate corrections, but the uncertainties associated with those corrections were inordinately large (DOE 1997). These circumstances were a long-term source of frustration in data analysis. For example, implementation of a casing correction required the data analyst to choose either the correction for the casing thickness that was closest to the actual thickness, accompanied by a small uncertainty and an unknown systematic error (caused by the thickness mismatch), or the correction for the actual thickness, accompanied by a large uncertainty. The revamped corrections were deduced by linear interpolation of the parameters in the correction equations. The corrections are accurate and the uncertainties are small.

The new calibration factors and field verification acceptance criteria are presented in Tables 1-2, 1-3, and 1-4 in Sections 1.2 and 1.3 for the data analysts' convenient reference.

Later sections in this report give details about the calibration data, data analyses, stabilities of system performances over time, and casing and water-filled borehole corrections. Section 2.2 describes data acquisition, and Section 2.3 summarizes the data processing that produced the revised calibration factors. Comparisons of representative new calibration results with those of prior calibrations appear in Section 4.0.

## 1.2 Calibration Function

The SGLS calibration is embodied in a calibration function,  $I(E)$ . For a particular gamma-ray energy  $E$  the value of the function is the ratio of the gamma-ray source intensity to the intensity of the associated peak in the gamma-ray spectrum.

$$I(E) = \frac{\text{source intensity for gamma ray with energy } E}{\text{intensity of associated spectral peak}}. \quad (1-1)$$

Representative values of the function can be easily determined from calibration measurements. The source intensity (in gammas per second per gram) for a particular gamma ray and a particular calibration standard is calculated from the known source concentration (in picocuries per gram) and gamma-ray yield (in gammas per decay). The calibration standard is logged several times to obtain gamma-ray spectra, and the intensities (in counts per second) of the spectral peaks associated with the

particular gamma ray are compiled. The peak intensities are corrected for dead time, and the average intensity is determined. The value of the calibration function is then calculated by dividing the source intensity by the average spectral peak intensity.

The calibration standards contain potassium, radium (uranium), and thorium gamma-ray sources that emit gamma rays with energies ranging from less than 200 keV to more than 2600 keV. Calibration measurements therefore yield spectra with peaks corresponding to the numerous gamma-ray energies. From the measured peak intensities and the known source intensities, values of the calibration function can be determined for the many discrete gamma-ray energies.

Previous calibrations determined that the calibration function can be represented by

$$I(E) = (C + D \ln(E))^2, \quad (1-2)$$

in which  $C$  and  $D$  are calibration constants and the independent variable  $E$  is the gamma-ray energy. At each recalibration,  $I(E)$  values are calculated using Equation (1-1) and the calibration data, then revised values for the two calibration constants are derived by analyzing the  $I(E)$  values and associated gamma energies with the *TableCurve* (trademark of Jandel Scientific, San Rafael, California) curve fitting program.

In data analysis, the calibration function is used directly to determine the intensity of any gamma-emitting source surrounding a borehole. The borehole is logged and the intensity of the appropriate peak in the spectrum is calculated and corrected for dead time. The product of the corrected peak intensity and the value of the calibration function for the particular energy is the source intensity. The source concentration is easily calculated from the source intensity.

The calibration function is used for all gamma-ray sources, natural or man-made. The accuracy of a gamma-ray source concentration calculated with this function depends on several factors, the most important of which may be the distribution of the source in the subsurface. Every calibration spectrum was collected with the detector surrounded by a large homogeneous volume of source-bearing material, so the calibration results are optimized to this source-detector configuration. Source concentrations calculated from field data will therefore be most accurate when the gamma-ray sources in the subsurface are similarly distributed.

Table 1-2 displays the new values for  $C$  and  $D$ . These values are appropriate if  $E$  is in kilo-electron-volt units and  $I(E)$  is expressed in gammas per second per gram per count per second.

*Table 1-2. Constants for the Calibration Function*

Logging System	$C \pm 2s C^1$	$D \pm 2s D$	Effective Dates
Gamma 2A	$0.0095 \pm 0.0050$	$0.01876 \pm 0.00076$	11/04/1999
Gamma 2B	$0.0237 \pm 0.0058$	$0.01453 \pm 0.00088$	10/04/1999



<sup>1</sup> The notation “2s C” denotes the two-sigma uncertainty in C.

To determine the concentration of a gamma-ray emitter, one calculates the value of  $I(E)$  at the particular gamma-ray energy using Equation (1-2) and the constants  $C$  and  $D$  appropriate for the logging system. By definition,  $I(E)$  is the ratio of the gamma-ray source intensity to the corresponding (corrected) spectral peak intensity  $P$ , so the intensity of the gamma-ray source  $S$ , in gamma rays per second per gram (γ/s/g), is the product of  $I(E)$  and  $P$ :

$$S = I(E)P. \quad (1-3)$$

The concentration of the gamma-ray source is

$$\text{concentration} = \frac{27.027}{Y} S = \frac{27.027}{Y} I(E)P. \quad (1-4)$$

In Equation (1-4),  $Y$  is the gamma-ray yield in gamma rays per decay, and the conversion  $27.027 \text{ pCi} = 1 \text{ decay per second}$  accounts for the factor 27.027.

### 1.3 Revised Field Verification Acceptance Criteria

A logging run produces a set of borehole measurements recorded sequentially in depth and time with the data acquisition parameters held constant. The logging of a borehole may require one or several logging runs. In routine operations, at least one field verification spectrum is recorded before each logging run, and at least one additional spectrum is recorded upon completion of the run. The gamma-ray sources for field verification are Amersham *KUTH Field Verifier* sources.

Before the sixth recalibration, acceptance tolerances were derived and used by methods described in Section 4.0 of DOE (1988b). After the sixth recalibration, those methods were replaced with a two-tier acceptance test based on conventional control chart practice. Both peak intensity and FWHM for the three spectral peaks associated with the 609.3-keV, 1460.8-keV, and 2614.5-keV gamma rays are compared to *warning limits* and *control limits* derived from the two-sigma and three-sigma deviations from the mean values. A logging system passes the acceptance test if all six of the parameters (three peak intensities and three FWHM) of a field verification spectrum lie within corresponding warning limits. If one of the six parameter values falls outside of the warning limits for the parameter, the next verification spectrum is examined, and if the same parameter value also falls outside the warning limits, on the same side of the limit range as the first discrepancy, the acceptance test is failed. If the same parameter value falls outside the warning limits, but on the opposite side of the limit range, then a third spectrum must be examined. If the same parameter from the third spectrum also lies outside the warning limit, then the acceptance test is failed.

A logging system malfunction is assumed if a field verification reading falls outside the control limits. In other words, if any FWHM or peak intensity value lies outside of the control limits, the logging system fails the acceptance test.

Warning and control limits for Gamma 2A and Gamma 2B are listed in Tables 1-3 and 1-4. These acceptance criteria are applicable until new acceptance criteria are established by the next recalibration.

Section 5.0 presents additional details about these criteria.

The criteria for Gamma 1A and Gamma 1B were not updated because these logging systems were not recalibrated in 1999.

*Table 1-3. Field Verification Acceptance Criteria for Gamma 2A <sup>1</sup>*

Gamma-Ray Energy (keV)	Parameter	Warning Limits		Control Limits	
		Lower	Upper	Lower	Upper
609.3	Peak intensity	7.55 c/s	8.96 c/s	7.20 c/s	9.31 c/s
	FWHM	1.67 keV	1.85 keV	1.63 keV	1.90 keV
1460.8	Peak intensity	8.57 c/s	10.04 c/s	8.21 c/s	10.41 c/s
	FWHM	2.08 keV	2.37 keV	2.01 keV	2.44 keV
2614.5	Peak intensity	1.79 c/s	2.18 c/s	1.69 c/s	2.28 c/s
	FWHM	2.48 keV	3.15 keV	2.32 keV	3.32 keV

<sup>1</sup> These criteria are applicable between September 22, 1998 (the last day upon which field verification spectra were recorded in the field) and the establishment of new criteria at the next recalibration.

*Table 1-4. Field Verification Acceptance Criteria for Gamma 2B <sup>1</sup>*

Gamma-Ray Energy (keV)	Parameter	Warning Limits		Control Limits	
		Lower	Upper	Lower	Upper
609.3	Peak intensity	8.53 c/s	9.90 c/s	8.19 c/s	10.24 c/s
	FWHM	1.71 keV	1.84 keV	1.68 keV	1.88 keV
1460.8	Peak intensity	10.16 c/s	11.69 c/s	9.78 c/s	12.08 c/s
	FWHM	2.12 keV	2.32 keV	2.07 keV	2.36 keV
2614.5	Peak intensity	2.19 c/s	2.58 c/s	2.09 c/s	2.68 c/s
	FWHM	2.53 keV	3.02 keV	2.41 keV	3.14 keV

<sup>1</sup> These criteria are applicable between December 10, 1999 and the establishment of new criteria at the next recalibration.

## 1.4 Revised Corrections for Casing and Water-Filled Boreholes

Casing corrections and corrections for water-filled boreholes were first developed from measurements conducted at the base calibration (DOE 1995b). The corrections were formulated for implementation by the standard method; an analyst would multiply the spectral peak intensity by the correction to get the corrected intensity. Data used to determine corrections were acquired through measurements that were constrained by limited test apparatus. In particular, only four sections of test casing were

available; these had wall thicknesses of 0.250 inches, 0.330 inches, 0.375 inches, and 0.650 inches. The 0.330-inch-thick casing fit inside of the 0.650-inch-thick casing, allowing measurements for the thickness of 0.980 inches. Similarly, water-filled borehole measurements were limited to borehole diameters of 4.5 inches, 7.0 inches, 9.0 inches, and 12.0 inches. These are the diameters of test holes in the DOE-GJO KW Model.

None of the casing thicknesses or borehole diameters used for the correction measurements matched the corresponding parameters of the Hanford boreholes. However, the corrections followed trends that could be accurately simulated by simple mathematical expressions. For example, curve-fitting analysis (DOE 1995b) showed that the casing correction  $K(E)$  could be calculated for any observed gamma-ray energy  $E$  with

$$K(E) = \frac{1}{A_C \% \frac{B_C}{\ln(E)}}, \quad (1-5)$$

in which  $A_C$  and  $B_C$  are constants for a particular casing thickness. Although Equation (1-5) and the  $A_C$  and  $B_C$  values derived from the base calibration data yielded corrections limited to the five test casing thicknesses, it seemed reasonable to expect that corrections for the thicknesses encountered in the Hanford boreholes could be obtained by curve fitting  $A_C$  and  $B_C$  with borehole diameter as the variable. In fact, curve-fitting did give corrections for the required thicknesses, but these corrections had uncertainties that were much larger than the uncertainties associated with the directly measured corrections (DOE 1997).

The large uncertainties accompanying the curve-fitted corrections were artifacts of the analysis and were undesirable because they produced large uncertainties in the gamma-ray source concentrations that were derived from corrected peak intensities. Large uncertainties in source concentrations obviously hamper environmental monitoring. If a borehole log and a re-log both yield concentrations with huge uncertainties, it might be difficult to decide if the concentration has changed or remained stable during the time between log runs.

The fact that most of the Hanford borehole parameter values lay between two experimental parameter values suggested the possibility of using linear interpolation. For example, the most common Hanford casing thickness, 0.280 inches, is between the two thicknesses of 0.250 inches and 0.330 inches for which measurements were made. Thus, for example, linear interpolation between the  $A_C$  and  $B_C$  values for 0.250 inches and 0.330 inches might yield accurate  $A_C$  and  $B_C$  values for the 0.280-inch thickness if the  $A_C$  and  $B_C$  values were nearly linear in relation to casing thickness.

Appendix A explains how linear interpolation was used to derive values of  $A_C$  and  $B_C$  appropriate for the three casing thicknesses most prevalent at Hanford. A fourth thickness, 0.237 inches, was outside of the range spanned by the test casing thicknesses. However, values of  $A_C$  and  $B_C$  for this thickness were derived by linear extrapolation. Tables 1-5 and 1-6 display the  $A_C$  and  $B_C$  values. These values, together with Equation (1-5), produce accurate corrections with reasonable uncertainties.

*Table 1-5. Casing Correction Parameters for Gamma 1A<sup>1</sup>*

Casing Thickness (inches)	$A_c$	$B_c$
0.237	$1.4872 \pm 0.0044$	$-5.455 \pm 0.027$
0.280	$1.5030 \pm 0.0026$	$-5.838 \pm 0.016$
0.322	$1.5184 \pm 0.0028$	$-6.212 \pm 0.016$
0.365	$1.5124 \pm 0.0030$	$-6.339 \pm 0.018$

<sup>1</sup> The parameters for Gamma 1B are assumed to be identical.

*Table 1-6. Casing Correction Parameters for Gamma 2A<sup>1</sup>*

Casing Thickness (inches)	$A_c$	$B_c$
0.237	$1.5233 \pm 0.0093$	$-5.742 \pm 0.056$
0.280	$1.4953 \pm 0.0053$	$-5.828 \pm 0.032$
0.322	$1.4680 \pm 0.0045$	$-5.912 \pm 0.027$
0.365	$1.4744 \pm 0.0040$	$-6.123 \pm 0.023$

<sup>1</sup> The parameters for Gamma 2B are assumed to be identical.

Corrections for water-filled boreholes were also established from measurements taken at the base calibration (DOE 1995b). It was shown that a correction for a particular gamma-ray energy  $E$  could be calculated with

$$K(E) = \sqrt{A_w \% \frac{B_w}{E}}. \quad (1-6)$$

In Equation (1-6),  $A_w$  and  $B_w$  are parameters that take constant values for a particular borehole diameter.

As indicated at the beginning of Section 1.4, values for  $A_w$  and  $B_w$  were determined for four borehole diameters that did not match any of the diameters of boreholes at Hanford. An investigation similar to the one followed for casing corrections led to the conclusion that values for  $A_w$  and  $B_w$  for the Hanford boreholes could be established by applying linear interpolation to the  $A_w$  and  $B_w$  that were derived from the base calibration measurements. Interpolated  $A_w$  and  $B_w$  values for the most common borehole diameters at Hanford are displayed in Table 1-7 for Gamma 2A. These values yield accurate corrections with reasonable uncertainties.

*Table 1-7. Gamma 2A Water Correction Parameter Values for the Most Common Borehole Diameters at Hanford*

<b>Borehole Inner Diameter (inches)</b>	<b><math>A_w</math></b>	<b><math>B_w</math></b>
4.0	$1.1210 \pm 0.0040$	$-52.8 \pm 2.8$
6.0	$1.5290 \pm 0.0085$	$673.1 \pm 6.6$
8.0	$1.768 \pm 0.015$	$1845 \pm 12$
10.0	$1.069 \pm 0.060$	$4797 \pm 53$

No values for Gamma 1A are reported because a re-investigation of the water corrections that was undertaken for the sixth recalibration (DOE 1999) indicated that the water correction data taken with Gamma 1A at the base calibration were affected by an electronics problem that appeared only when the sonde was immersed. Therefore, at present all data from water-filled borehole logs are being corrected with corrections calculated with Equation (1-6) and the parameters in Table 1-7.

Appendix B provides details about the water correction investigations.

## 2.0 Revised Calibration Functions

### 2.1 Calibration Standards

Calibration measurements were conducted by logging borehole calibration standards at Hanford. The standards and their links to New-Brunswick-Laboratory-certified standards, and other standards, are described in Heistand et al. (1984) and Leino et al. (1994). The names of the borehole standards and their source “concentrations” (actually, decay rates per unit mass) are displayed in Table 2-1.

*Table 2-1. Calibration Standards and Their Source Concentrations*

<b>Standard</b>	<b><sup>40</sup>K Concentration (pCi/g)</b>	<b><sup>226</sup>Ra Concentration <sup>1</sup> (pCi/g)</b>	<b><sup>232</sup>Th Concentration (pCi/g)</b>
SBK <sup>2,3</sup>	53.50 ± 1.67	1.16 ± 0.11	0.11 ± 0.02
SBU <sup>2,3</sup>	10.72 ± 0.84	190.52 ± 5.81	0.66 ± 0.06
SBT <sup>2,3</sup>	10.63 ± 1.34	10.02 ± 0.48	58.11 ± 1.44
SBM <sup>2,3</sup>	41.78 ± 1.84	125.79 ± 4.00	39.12 ± 1.07
SBA <sup>3</sup>	undetermined	61.2 ± 1.7	undetermined
SBL <sup>3</sup>	undetermined	324 ± 9	undetermined
SBB <sup>3</sup>	undetermined	902 ± 27	undetermined

<sup>1</sup> If <sup>226</sup>Ra is in decay equilibrium with <sup>238</sup>U, then the concentrations (decay rates) of the two nuclides are equal.

<sup>2</sup> Standards used for calibration.

<sup>3</sup> Standards used for linearity checks.

Table 2-2 lists the gamma-ray counting standards to which the source concentrations in the borehole standards are referenced.

*Table 2-2. Reference Standards for Calibration Standard Source Concentrations*

<b>Source</b>	<b>Reference Standard</b>
Potassium ( <sup>40</sup> K)	reagent-grade potassium carbonate (K <sub>2</sub> CO <sub>3</sub> )
Radium ( <sup>226</sup> Ra)	NBL (New Brunswick Laboratory) 100-A Series Uranium <sup>1</sup>
Thorium ( <sup>232</sup> Th)	NBL 100-A Series Thorium <sup>1</sup>

<sup>1</sup> Trahey et al. (1982).

Reports for previous recalibrations (e.g., DOE 1998b) acknowledged that the pores in the calibration standard materials contain unknown concentrations of water, but the source concentrations are reported in terms of decay activity *per unit dry mass* (Leino et al. 1994). This means that the constants *C* and *D* in the calibration equation (Equation (1-2)) are calculated with *concentrations based on dry mass* and *spectral peak intensities from water-bearing standards*. If the subsurface in the Hanford Tank Farms contained the same percentage of water as the calibration standards, then the calibration and the log measurements would both involve water-bearing media. The radionuclide

concentrations calculated with the calibration function would be in terms of decay activity per unit dry mass, and would be accurate.

However, most logging in the Tank Farms interrogates *unsaturated* media. Because there is no way to remove the water from the pore spaces in the calibration standards, it is not possible to match the calibration condition to the normal field condition. All that can be done is to estimate the largest potential error that could result from the water content mismatch between calibration standard and logged medium. A study documented in Section 2.0 of DOE (1999) indicates that the maximum systematic error would be overestimation of concentrations by about 14 percent.

## 2.2 Data Acquisition

Each spectrum for calibration and linearity confirmations was acquired with the sonde held stationary and centered in the dry, open (uncased) test hole of the particular calibration standard. For each test configuration, six spectra were acquired with an acquisition time of 1,000 seconds per spectrum.

## 2.3 Data Analysis

Spectra were analyzed with version 6.3.1, release 13 of the spectrum analysis program *PCMCA/WIN* (Aptec Engineering Limited, North Tonawanda, New York). All of the user-specified software settings were identical to those customarily used for analysis of field data. The analysis method used for field data was applied, with two exceptions. First, whereas field spectra are normally energy-calibrated by “importing” an energy calibration from a field verification spectrum, the calibration spectra were individually calibrated for energy using spectral peaks associated with some of the following gamma rays: 295.2 keV ( $^{214}\text{Pb}$ , uranium series), 609.3 keV ( $^{214}\text{Bi}$ , uranium series), 1120.3 keV ( $^{214}\text{Bi}$ , uranium series), 1460.8 keV ( $^{40}\text{K}$ ), 1764.5 keV ( $^{214}\text{Bi}$ , uranium series), 2204.1 keV ( $^{214}\text{Bi}$ , uranium series), and 2614.5 keV ( $^{208}\text{Tl}$ , thorium series). Second, whereas field spectra are usually resolution-calibrated by importing a resolution calibration from a field verification spectrum, the calibration spectra were individually calibrated for resolution using the *resolution calibration* algorithm in *PCMCA/WIN*.

Spectral peaks were identified using the *PCMCA/WIN peaksearch* algorithm, and the peak areas were calculated with the *multifit* algorithm. The peak areas calculated by the *multifit* algorithm were the (numerical) integrals of Gaussian functions that were fitted to the peaks using resolution calibration functions that were manually determined for each spectrum, as described in Section 5.0 of DOE (1998). The peak intensities, denoted by  $P$  and expressed in counts per second, were calculated by dividing each peak area by the counting time over which the spectrum was acquired. All of the peak intensities were corrected for the logging system dead time by the method described in Section 3.0.

Because six spectra were acquired for each calibration standard, there were generally six peak intensities for each significant gamma ray associated with a calibration standard. Each set of six intensities was examined for entries that differed significantly from the mean of the set. These “outliers” were eliminated from the data sets if the deletions were justified by the Chauvenet criterion (Friedlander et al. 1981). According to this criterion, rejection of a datum is justified if the difference between the datum and the data set mean has a probability of occurrence that is less than  $1/(2N)$ , where  $N$  is the

number of elements in the set. The probability is calculated under the assumption that the data are normally distributed.

The weighted average for each set of dead-time-corrected intensities (with outliers removed) was calculated and used as the representative intensity. The weighted average intensity was calculated using

$$\text{weighted average } P = \langle P \rangle = \frac{\sum_{i=1}^6 P_i @ w_i}{\sum_{i=1}^6 w_i}. \quad (2-1)$$

Each weight  $w_i$  in Equation (2-1) is the inverse square of the associated peak intensity uncertainty (95 percent confidence or 2s uncertainty):

$$w_i = \frac{1}{(2s P_i)^2}. \quad (2-2)$$

The 2s uncertainty in  $\langle P \rangle$  was calculated as follows:

$$2s \langle P \rangle = \frac{1}{\sqrt{\sum_{i=1}^6 w_i}}. \quad (2-3)$$

The calibration model source intensities are displayed in Table 2-3, and average intensities for representative peaks are displayed in Tables 2-4 and 2-5.



*Table 2-3. Calibration Model Source Intensities*

<b>Gamma-Ray Energy (keV)</b>	<b>SBK Source Intensity (<math>\mu\text{s/g}</math>) per (c/s)</b>	<b>SBU Source Intensity (<math>\mu\text{s/g}</math>) per (c/s)</b>	<b>SBT Source Intensity (<math>\mu\text{s/g}</math>) per (c/s)</b>	<b>SBM Source Intensity (<math>\mu\text{s/g}</math>) per (c/s)</b>
129.1	0.00012 $\pm$ 0.00002	0.0007 $\pm$ 0.0001	0.0630 $\pm$ 0.0016	0.0424 $\pm$ 0.0012
185.9	0.00253 $\pm$ 0.00017	0.4152 $\pm$ 0.0090	0.0218 $\pm$ 0.0007	0.2741 $\pm$ 0.0062
238.6	0.00175 $\pm$ 0.00032	0.0105 $\pm$ 0.0010	0.927 $\pm$ 0.023	0.624 $\pm$ 0.017
241.9	0.00336 $\pm$ 0.00031	0.528 $\pm$ 0.016	0.1115 $\pm$ 0.0025	0.404 $\pm$ 0.011
270.3	0.00044 $\pm$ 0.00004	0.0474 $\pm$ 0.0014	0.0835 $\pm$ 0.0020	0.0853 $\pm$ 0.0018
277.4	0.00010 $\pm$ 0.00002	0.0006 $\pm$ 0.0001	0.0503 $\pm$ 0.0012	0.0339 $\pm$ 0.0009
295.2	0.00825 $\pm$ 0.00078	1.355 $\pm$ 0.041	0.0712 $\pm$ 0.0034	0.894 $\pm$ 0.028
300.1	0.00022 $\pm$ 0.00002	0.0156 $\pm$ 0.0003	0.0711 $\pm$ 0.0017	0.0571 $\pm$ 0.0013
328.0	0.00014 $\pm$ 0.00002	0.0008 $\pm$ 0.0001	0.0722 $\pm$ 0.0018	0.0486 $\pm$ 0.0013
338.4	0.00049 $\pm$ 0.00009	0.0029 $\pm$ 0.0003	0.2582 $\pm$ 0.0064	0.1738 $\pm$ 0.0048
352.0	0.0162 $\pm$ 0.0015	2.657 $\pm$ 0.080	0.1397 $\pm$ 0.0066	1.754 $\pm$ 0.055
583.1	0.00127 $\pm$ 0.00023	0.0076 $\pm$ 0.0007	0.669 $\pm$ 0.016	0.450 $\pm$ 0.012
609.3	0.0198 $\pm$ 0.0019	3.249 $\pm$ 0.099	0.1709 $\pm$ 0.0082	2.145 $\pm$ 0.068
727.1	0.00051 $\pm$ 0.00009	0.0031 $\pm$ 0.0003	0.2709 $\pm$ 0.0063	0.1824 $\pm$ 0.0047
768.4	0.00209 $\pm$ 0.00020	0.344 $\pm$ 0.010	0.0181 $\pm$ 0.0009	0.2271 $\pm$ 0.0072
785.4	0.00008 $\pm$ 0.00002	0.0005 $\pm$ 0.0000	0.0430 $\pm$ 0.0011	0.0289 $\pm$ 0.0008
794.8	0.00020 $\pm$ 0.00004	0.0012 $\pm$ 0.0001	0.1041 $\pm$ 0.0026	0.0701 $\pm$ 0.0019
860.5	0.00018 $\pm$ 0.00003	0.0011 $\pm$ 0.0001	0.0929 $\pm$ 0.0023	0.0626 $\pm$ 0.0017
911.1	0.00118 $\pm$ 0.00021	0.0072 $\pm$ 0.0006	0.624 $\pm$ 0.016	0.420 $\pm$ 0.012
934.1	0.00136 $\pm$ 0.00013	0.2228 $\pm$ 0.0068	0.0117 $\pm$ 0.0006	0.1471 $\pm$ 0.0047
964.6	0.00039 $\pm$ 0.00004	0.0283 $\pm$ 0.0008	0.1186 $\pm$ 0.0029	0.0967 $\pm$ 0.0022
968.9	0.00071 $\pm$ 0.00013	0.0043 $\pm$ 0.0004	0.3754 $\pm$ 0.0093	0.2527 $\pm$ 0.0069
1120.3	0.00646 $\pm$ 0.00061	1.060 $\pm$ 0.032	0.0558 $\pm$ 0.0027	0.700 $\pm$ 0.022
1238.1	0.00254 $\pm$ 0.00024	0.417 $\pm$ 0.013	0.0219 $\pm$ 0.0011	0.2753 $\pm$ 0.0088
1377.7	0.00173 $\pm$ 0.00016	0.2834 $\pm$ 0.0086	0.0149 $\pm$ 0.0007	0.1871 $\pm$ 0.0059
1408.0	0.00106 $\pm$ 0.00010	0.1746 $\pm$ 0.0053	0.0092 $\pm$ 0.0004	0.1153 $\pm$ 0.0037
1460.8	0.2118 $\pm$ 0.0066	0.0427 $\pm$ 0.0033	0.0644 $\pm$ 0.0053	0.1805 $\pm$ 0.0073
1509.2	0.00094 $\pm$ 0.00009	0.1545 $\pm$ 0.0047	0.0081 $\pm$ 0.0004	0.1020 $\pm$ 0.0032
1587.9	0.00015 $\pm$ 0.00003	0.0009 $\pm$ 0.0001	0.0798 $\pm$ 0.0020	0.0537 $\pm$ 0.0015
1620.6	0.00011 $\pm$ 0.00002	0.0007 $\pm$ 0.0001	0.0591 $\pm$ 0.0015	0.0398 $\pm$ 0.0011
1729.6	0.00131 $\pm$ 0.00012	0.2150 $\pm$ 0.0066	0.0113 $\pm$ 0.0005	0.1418 $\pm$ 0.0045
1764.5	0.00683 $\pm$ 0.00065	1.122 $\pm$ 0.034	0.0590 $\pm$ 0.0028	0.741 $\pm$ 0.024
1847.4	0.00091 $\pm$ 0.00009	0.1497 $\pm$ 0.0046	0.0079 $\pm$ 0.0004	0.0988 $\pm$ 0.0031
2204.1	0.00214 $\pm$ 0.00020	0.352 $\pm$ 0.011	0.0185 $\pm$ 0.0009	0.2324 $\pm$ 0.0074
2614.5	0.00147 $\pm$ 0.00027	0.0088 $\pm$ 0.0008	0.774 $\pm$ 0.019	0.521 $\pm$ 0.014

*Table 2-4. Calibration Peak Intensities Recorded by Gamma 2A*

<b>Gamma-Ray Energy (keV)</b>	<b>SBK Weighted Average Peak Intensities ( counts per second)</b>	<b>SBU Weighted Average Peak Intensities ( counts per second)</b>	<b>SBT Weighted Average Peak Intensities ( counts per second)</b>	<b>SBM Weighted Average Peak Intensities ( counts per second)</b>
129.1	no data	no data	2.91 ± 0.25	no data
185.9	no data	34.21 ± 0.33	no data	22.58 ± 0.29
238.6	no data	3.46 ± 0.72	74.0 ± 3.5	49.2 ± 1.1
241.9	no data	41.47 ± 0.77	no data	49.3 ± 2.1
270.3	no data	3.8 ± 1.0	6.00 ± 0.13	5.78 ± 0.25
277.4	no data	2.38 ± 0.99	3.67 ± 0.12	no data
295.2	no data	99.8 ± 1.5	5.67 ± 0.14	65.9 ± 1.1
300.1	no data	no data	5.50 ± 0.15	4.22 ± 0.72
328.0	no data	no data	4.68 ± 0.22	2.94 ± 0.35
338.4	no data	no data	17.67 ± 0.37	11.73 ± 0.32
352.0	0.59 ± 0.03	186.7 ± 2.9	10.31 ± 0.16	122.6 ± 1.5
583.1	no data	no data	38.64 ± 0.33	25.20 ± 0.42
609.3	0.70 ± 0.03	190.1 ± 2.6	10.34 ± 0.13	124.9 ± 1.8
727.1	no data	no data	8.91 ± 0.10	5.80 ± 0.13
768.4	no data	19.86 ± 0.54	1.07 ± 0.06	12.32 ± 0.27
785.4	no data	4.50 ± 0.10	1.46 ± 0.07	3.72 ± 0.10
794.8	no data	no data	5.17 ± 0.11	3.37 ± 0.10
860.5	no data	no data	5.32 ± 0.07	3.62 ± 0.08
911.1	no data	no data	31.04 ± 0.22	20.44 ± 0.26
934.1	no data	11.74 ± 0.11	0.64 ± 0.05	7.55 ± 0.09
964.6	no data	1.17 ± 0.19	5.89 ± 0.11	4.63 ± 0.08
968.9	no data	no data	18.78 ± 0.18	12.40 ± 0.11
1120.3	0.21 ± 0.03	55.26 ± 0.68	2.96 ± 0.06	36.21 ± 0.39
1238.1	no data	21.16 ± 0.25	1.10 ± 0.05	13.83 ± 0.13
1377.7	no data	14.70 ± 0.13	0.80 ± 0.04	9.61 ± 0.10
1408.0	no data	8.41 ± 0.10	no data	5.56 ± 0.08
1460.8	7.53 ± 0.18	2.21 ± 0.08	2.65 ± 0.15	8.98 ± 0.17
1509.2	no data	7.51 ± 0.11	0.34 ± 0.04	4.75 ± 0.08
1587.9	no data	no data	3.30 ± 0.05	2.28 ± 0.13
1620.6	no data	no data	1.56 ± 0.04	0.97 ± 0.06
1729.6	0.05 ± 0.01	10.10 ± 0.11	0.50 ± 0.03	6.36 ± 0.07
1764.5	0.20 ± 0.01	52.82 ± 0.80	2.79 ± 0.05	34.61 ± 0.43
1847.4	no data	6.91 ± 0.10	0.41 ± 0.05	4.49 ± 0.07
2204.1	0.06 ± 0.01	15.81 ± 0.26	0.83 ± 0.04	10.08 ± 0.10
2614.5	0.04 ± 0.01	0.34 ± 0.02	30.84 ± 0.51	20.53 ± 0.30

*Table 2-5. Calibration Peak Intensities Recorded by Gamma 2B*

<b>Gamma-Ray Energy (keV)</b>	<b>SBK Weighted Average Peak Intensities (counts per second)</b>	<b>SBU Weighted Average Peak Intensities (counts per second)</b>	<b>SBT Weighted Average Peak Intensities (counts per second)</b>	<b>SBM Weighted Average Peak Intensities (counts per second)</b>
129.1	no data	no data	3.64 ± 0.38	no data
185.9	no data	40.07 ± 0.57	no data	25.66 ± 0.34
238.6	no data	4.64 ± 0.96	88.1 ± 3.6	58.0 ± 2.3
241.9	no data	48.23 ± 0.83	no data	56.5 ± 1.4
270.3	no data	4.84 ± 0.93	6.46 ± 0.19	6.44 ± 0.38
277.4	no data	2.7 ± 1.1	4.02 ± 0.20	2.9 ± 1.1
295.2	0.742 ± 0.042	120.8 ± 1.3	6.47 ± 0.17	75.9 ± 1.6
300.1	no data	no data	6.32 ± 0.17	5.2 ± 1.3
328.0	no data	no data	5.43 ± 0.20	3.57 ± 0.52
338.4	no data	no data	20.99 ± 0.38	13.58 ± 0.34
352.0	1.362 ± 0.050	225.4 ± 2.8	12.17 ± 0.14	146.3 ± 1.5
583.1	no data	no data	47.03 ± 0.41	30.55 ± 0.52
609.3	1.429 ± 0.034	234.4 ± 3.5	12.56 ± 0.13	152.2 ± 1.7
727.1	no data	no data	10.94 ± 0.12	6.99 ± 0.18
768.4	no data	25.04 ± 0.59	1.24 ± 0.06	15.08 ± 0.45
785.4	no data	5.62 ± 0.14	1.71 ± 0.08	4.48 ± 0.15
794.8	no data	no data	6.34 ± 0.14	4.19 ± 0.15
860.5	no data	no data	6.46 ± 0.09	4.19 ± 0.10
911.1	no data	no data	38.71 ± 0.24	25.00 ± 0.40
934.1	no data	14.76 ± 0.18	0.77 ± 0.06	9.45 ± 0.14
964.6	no data	1.64 ± 0.12	7.11 ± 0.11	5.54 ± 0.14
968.9	no data	no data	23.37 ± 0.21	15.34 ± 0.16
1120.3	0.407 ± 0.024	70.30 ± 0.95	3.67 ± 0.05	45.15 ± 0.75
1238.1	no data	26.90 ± 0.32	1.40 ± 0.05	17.31 ± 0.19
1377.7	no data	18.66 ± 0.24	0.99 ± 0.05	12.10 ± 0.17
1408.0	no data	10.77 ± 0.12	0.53 ± 0.08	7.03 ± 0.10
1460.8	13.96 ± 0.17	2.83 ± 0.10	3.43 ± 0.18	11.27 ± 0.17
1509.2	no data	9.43 ± 0.12	0.51 ± 0.03	5.96 ± 0.14
1587.9	no data	no data	4.17 ± 0.08	2.69 ± 0.15
1620.6	no data	no data	1.98 ± 0.06	1.22 ± 0.08
1729.6	0.072 ± 0.009	12.83 ± 0.19	0.66 ± 0.04	8.30 ± 0.11
1764.5	0.390 ± 0.015	68.4 ± 1.1	3.59 ± 0.06	44.05 ± 0.69
1847.4	0.056 ± 0.010	8.86 ± 0.10	0.40 ± 0.05	5.77 ± 0.08
2204.1	0.110 ± 0.007	20.49 ± 0.25	1.09 ± 0.04	13.13 ± 0.16
2614.5	0.076 ± 0.007	0.44 ± 0.02	39.80 ± 0.39	26.46 ± 0.37

Representative values of  $I(E)$  were calculated with Equation (1-1) and the source intensity values in Table 2-3 and the peak intensity values in Tables 2-4 and 2-5.

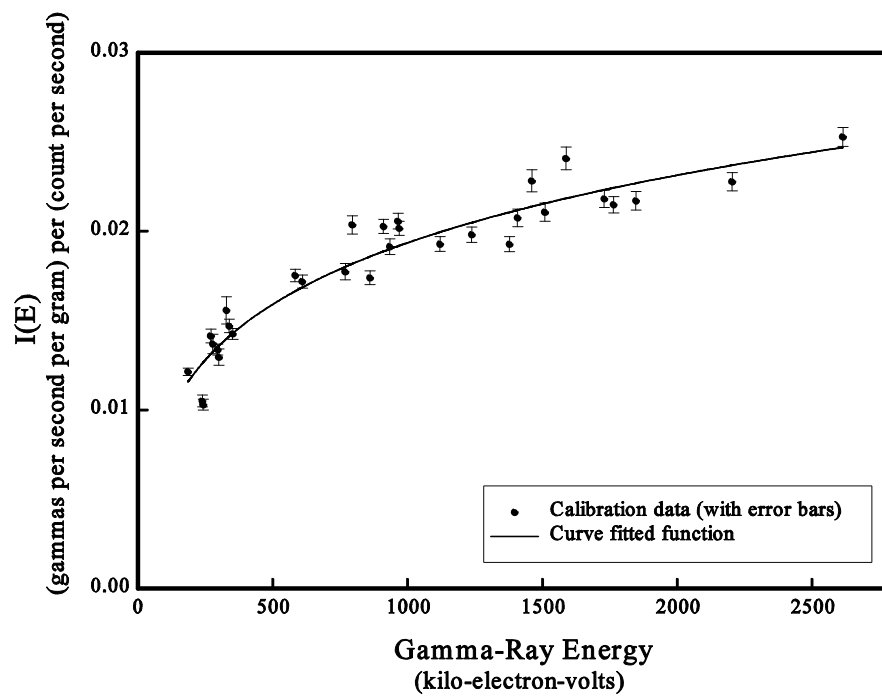


*Figure 2-1. Calibration Data and Calibration Function for Gamma 2A  
Plotted in Relation to Gamma-Ray Energy*

Symbols with error bars in Figure 2-1 represent the Gamma 2A calibration data plotted in relation to gamma-ray energy. The curve is the plot of the calibration function determined by curve fitting.

Plots for the Gamma 2B data and calibration function are shown in Figure 2-2.

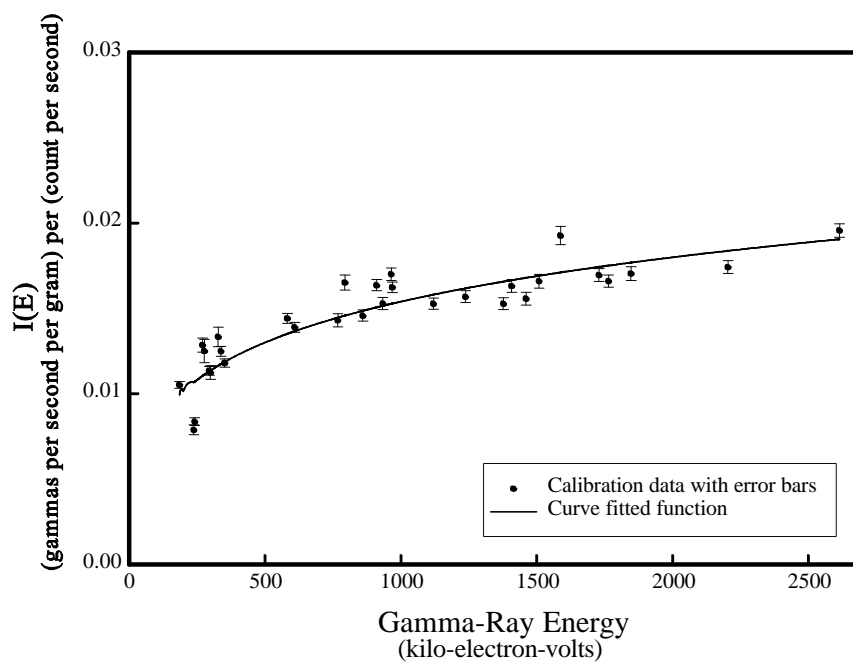


*Figure 2-2. Calibration Data and Calibration Function for Gamma 2B  
Plotted in Relation to Gamma-Ray Energy*

As mentioned in Section 1.2, curve-fitting to establish the calibration functions was done with the *TableCurve* program to determine values for  $C$  and  $D$  in Equation (1-2). Table 1-2 in Section 1.2 shows the revised values for  $C$  and  $D$  for Gamma 2A and Gamma 2B.

### 3.0 Linearity Test Results

As a consequence of the logging system dead time effect, the relationship between spectral peak intensities and gamma-ray source intensities is non-linear. The dead time correction was developed to offset the dead time effect, or to establish a linear relationship between dead-time-corrected peak intensities and intensities of the associated gamma-ray sources.

The study of the system dead time effect documented in the base calibration report (DOE 1995b) indicated that the effect of dead time on the intensity of a spectral peak could be offset by multiplying the peak intensity by a dead time correction:

$$\text{dead time correction} = \frac{1}{F \% G T_D \ln(T_D) \% H (T_D)^3}. \quad (3-1)$$

$T_D$  is the percent dead time and  $F$ ,  $G$ , and  $H$  are dimensionless factors that have constant values for a particular logging system. The values of  $F$ ,  $G$ , and  $H$  determined by the analysis of base calibration data are displayed in Table 3-1.

Table 3-1. Factors for the Dead Time Correction

Logging Unit	$F$	$G$	$H$
Gamma 1A Gamma 1B	$1.0080 \pm 0.0054$	$(-4.71 \pm 0.47) \times 10^{-4}$	$(-5.73 \pm 0.21) \times 10^{-7}$
Gamma 2A Gamma 2B	$1.0322 \pm 0.0022$	$(-1.213 \pm 0.028) \times 10^{-3}$	$(-1.89 \pm 0.20) \times 10^{-7}$

The dead time correction study indicated that the dead time corrections are independent of the gamma-ray energy.

The measurements that led to the dead time corrections for Gamma 1A and Gamma 2A have never been repeated, but the dead time corrections for all four systems have been indirectly validated at each recalibration using the fact that the dead time corrections establish linearity between corrected spectral peak intensities and gamma-ray source intensities. Thus, the validity of a dead time correction is confirmed if the relationship between corrected peak intensities and gamma-ray source concentrations is linear. These linearity demonstrations are part of each logging system recalibration.

For the seventh recalibration, spectra were acquired by logging all of the calibration standards listed in Table 2-1 with Gamma 2A and Gamma 2B. The spectral peak intensities for several “radium” gamma rays were corrected for dead time, then plotted in relation to  $^{226}\text{Ra}$  concentration.  $^{226}\text{Ra}$  concentrations ranged from 1.16 picocuries per gram to 902 picocuries per gram, and the system dead times ranged from less than one percent to slightly higher than 70 percent.

All of the data conformed to the expected linear relationships. Some examples are presented in peak-intensity-versus-source-concentration plots in Figures 3-1 through 3-6.

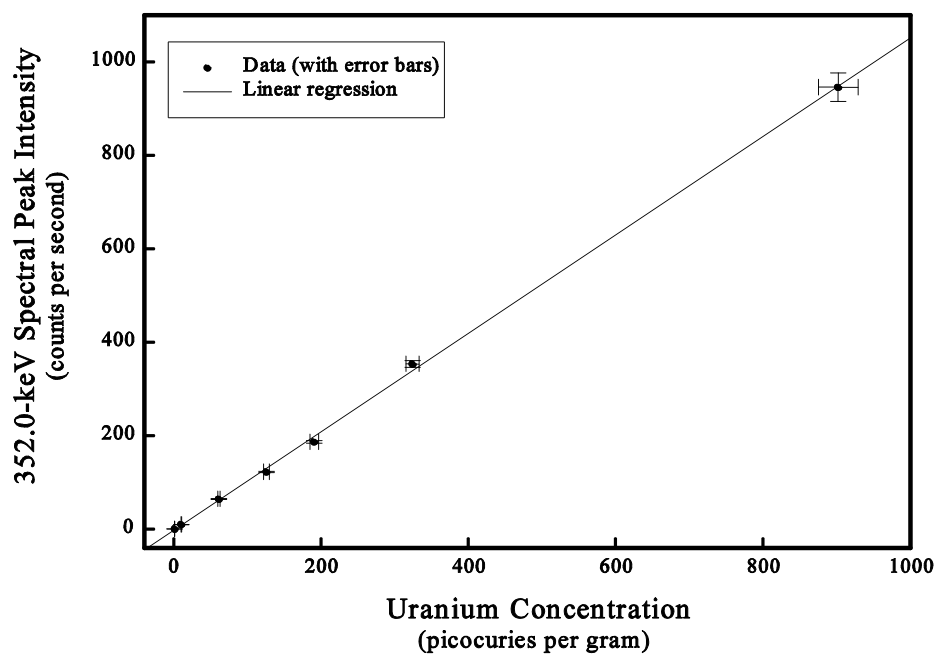


*Figure 3-1. Gamma 2A Linearity Demonstration for 352.0-keV Gamma-Ray Data*

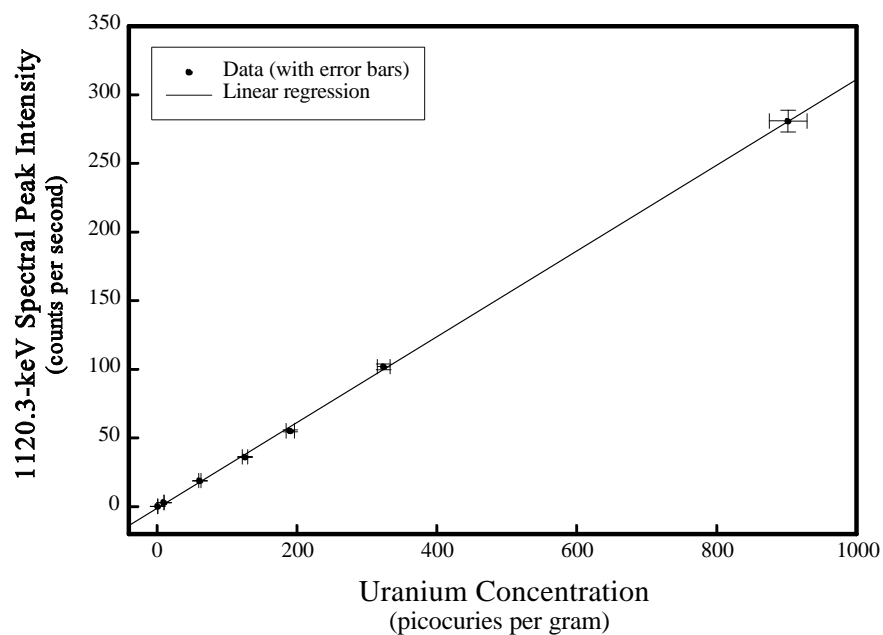


Figure 3-2. Gamma 2A Linearity Demonstration for 1120.3-keV Gamma-Ray Data

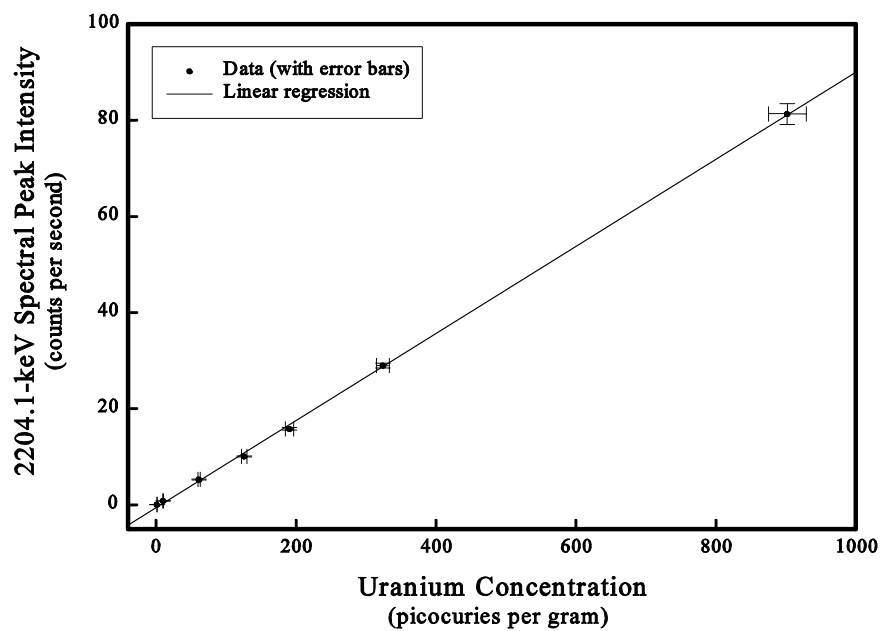


Figure 3-3. Gamma 2A Linearity Demonstration for 2204.1-keV Gamma-Ray Data



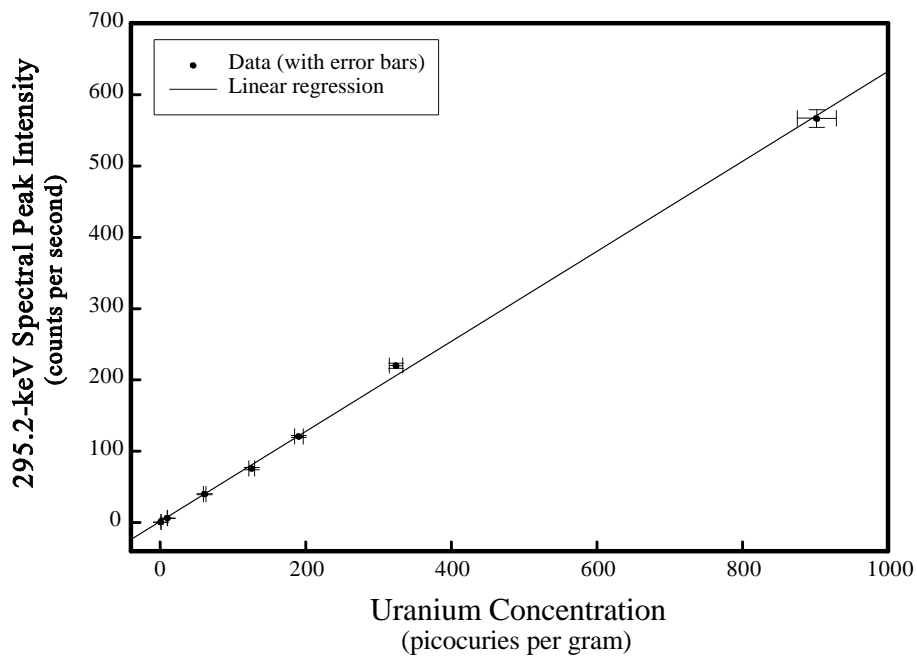


Figure 3-4. Gamma 2B Linearity Demonstration for 295.2-keV Gamma-Ray Data

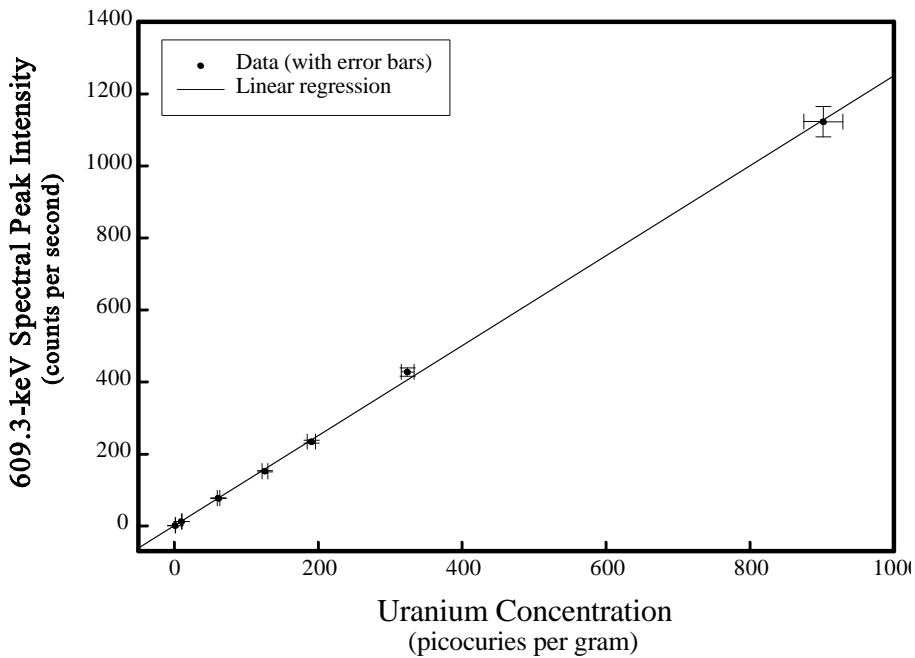
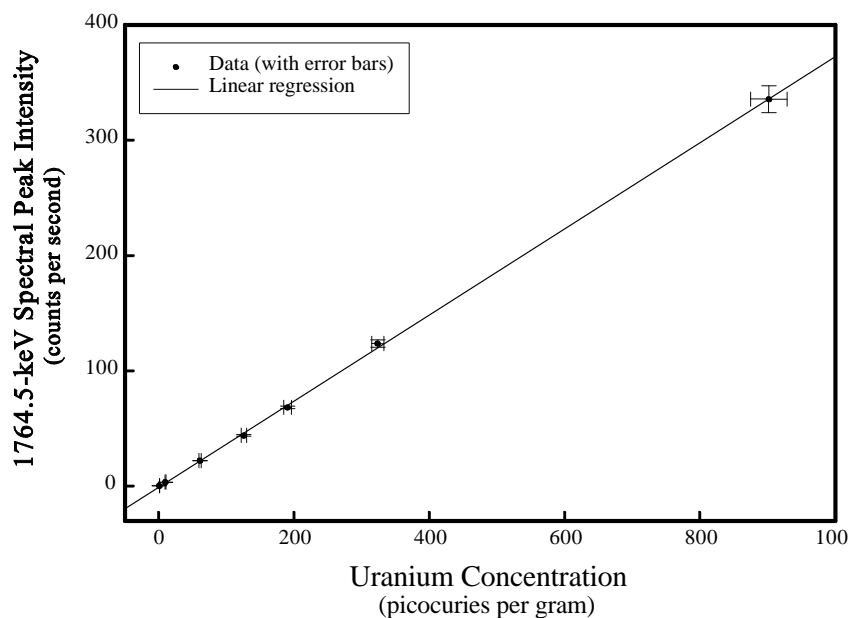


Figure 3-5. Gamma 2B Linearity Demonstration for 609.3-keV Gamma-Ray Data



*Figure 3-6. Gamma 2B Linearity Demonstration for 1764.5-keV Gamma-Ray Data*

Dead time data were acquired during the base calibration, but the backup sonde hadn't been acquired at that time. Thus, dead time corrections were never determined directly for Gamma 2B; log data taken with Gamma 2B have always been corrected with the Gamma 2A corrections. The graphs in Figures 3-4, 3-5, and 3-6 provide technical justification for this method. The application of the Gamma 2A dead time correction to data recorded with Gamma 2B yields corrected peak intensities that are linear in relation to gamma source concentration. This is seen to be true over a range of gamma-ray energies.

## 4.0 Comparison of Seventh Recalibration with Previous Recalibrations

Table 4-1 displays the calibration constants that have been determined over the lifetime of the project for the two Gamma 2 systems. Also displayed are values of the calibration function  $I(E)$  for energy values of 1460.8 keV ( $^{40}\text{K}$ ), 661.6 keV ( $^{137}\text{Cs}$ ), and 1173.2 keV ( $^{60}\text{Co}$ ). The  $I(E)$  values were calculated using Equation (1-2).

*Table 4-1. Calibration Constants and Sample  $I(E)$  Values for Gamma 2A and Gamma 2B*

Gamma 2A					
Calibration	$C$	$D$	$I(E)$ (gammas/second/gram) per (count/second)		
			E=1460.8 keV	E=661.6 keV	E=1173.2 keV
base	$0.0039 \pm 0.0058$	$0.01820 \pm 0.00083$	$0.0186 \pm 0.0023$	$0.0149 \pm 0.0019$	$0.0176 \pm 0.0022$
recal 1	$0.0092 \pm 0.0087$	$0.0174 \pm 0.0013$	$0.0185 \pm 0.0035$	$0.0149 \pm 0.0030$	$0.0175 \pm 0.0033$
recal 2	$0.0101 \pm 0.0088$	$0.0174 \pm 0.0013$	$0.0187 \pm 0.0035$	$0.0152 \pm 0.0030$	$0.0177 \pm 0.0034$
recal 3	$0.0131 \pm 0.0085$	$0.0172 \pm 0.0012$	$0.0192 \pm 0.0034$	$0.0156 \pm 0.0029$	$0.0181 \pm 0.0032$
recal 4	$0.0181 \pm 0.0035$	$0.01641 \pm 0.00053$	$0.0190 \pm 0.0014$	$0.0155 \pm 0.0012$	$0.0180 \pm 0.0014$
recal 5	$0.0165 \pm 0.0036$	$0.01665 \pm 0.00055$	$0.0190 \pm 0.0015$	$0.0155 \pm 0.0013$	$0.0180 \pm 0.0014$
recal 6	$0.0093 \pm 0.0053$	$0.01846 \pm 0.00080$	$0.0207 \pm 0.0023$	$0.0167 \pm 0.0019$	$0.0195 \pm 0.0022$
recal 7	$0.0095 \pm 0.0050$	$0.01876 \pm 0.00076$	$0.0214 \pm 0.0022$	$0.0173 \pm 0.0018$	$0.0202 \pm 0.0021$
Gamma 2B					
Calibration	$C$	$D$	$I(E)$ (gammas/second/gram) per (count/second)		
			E=1460.8 keV	E=661.6 keV	E=1173.2 keV
recal 4	$0.0310 \pm 0.0035$	$0.01305 \pm 0.00053$	$0.0159 \pm 0.0013$	$0.0134 \pm 0.0011$	$0.0152 \pm 0.0013$
recal 5	$0.0341 \pm 0.0033$	$0.01271 \pm 0.00050$	$0.0161 \pm 0.0012$	$0.0136 \pm 0.0011$	$0.0154 \pm 0.0012$
recal 6	$0.0242 \pm 0.0057$	$0.01433 \pm 0.00086$	$0.0165 \pm 0.0022$	$0.0138 \pm 0.0019$	$0.0157 \pm 0.0021$
recal 7	$0.0237 \pm 0.0058$	$0.01453 \pm 0.00088$	$0.0168 \pm 0.0022$	$0.0139 \pm 0.0019$	$0.0160 \pm 0.0021$

Note: No results prior to the fourth calibration are displayed for Gamma 2B because the backup sonde that is a component of Gamma 2B was acquired after the third recalibration.

The values of  $C$  and  $D$  and the associated value of  $I(E)$  for a particular calibration presumably quantify the efficiency of the logging system at the time of the calibration measurements. The entries in Table 4-1 indicate that for both logging systems the  $C$  and  $D$  values have changed over time to cause gradual increases in the associated  $I(E)$  values. The graph in Figure 4-1, in which Gamma 2A  $I(E)$  values for  $E = 1460.8$  keV are plotted in relation to time, illustrates the trend. The graph suggests that the variations in  $I(E)$  do not reflect random statistical scatter, but that  $I(E)$  has actually drifted upward over time. Because  $I(E)$  is the inverse of the system efficiency, the  $I(E)$  data indicate that both systems have experienced gradual decreases in efficiency.

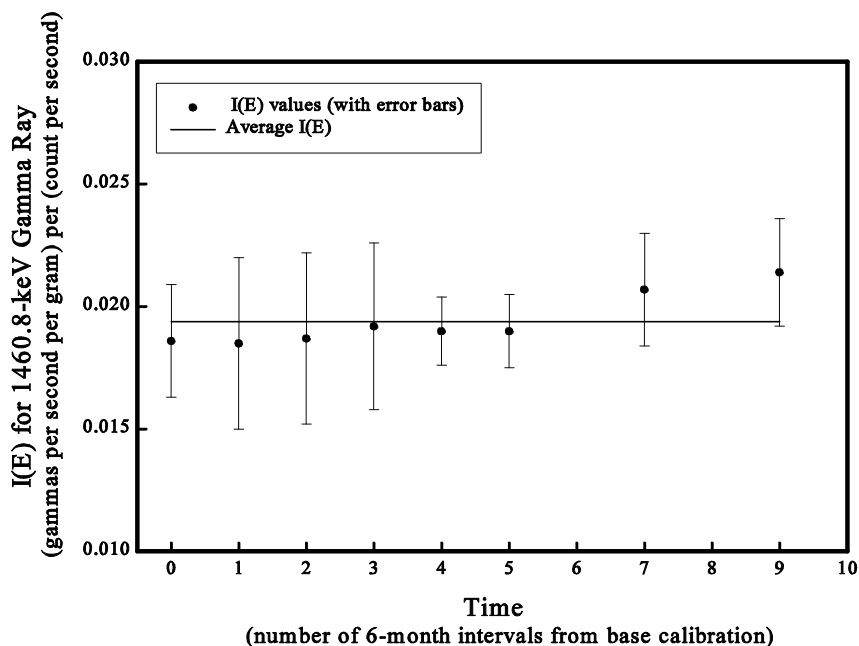


Figure 4-1. Variation of the 1460.8-keV Gamma 2A Calibration Function with Time

Two examples are presented as concrete illustrations of the effects of the efficiency drifts of Gamma 2A. The examples show how the efficiency changes affect calculated concentrations for two gamma-ray sources and associated gamma rays:

- C  $52.2 \pm 1.7$  picocuries  $^{40}\text{K}$  per gram (the  $^{40}\text{K}$  concentration in the DOE-GJO K Standard), 1460.8-keV gamma ray (energy just above the 1173.2-keV and 1332.5-keV  $^{60}\text{Co}$  gamma-ray energies).
- C  $162.9 \pm 5.3$  picocuries  $^{238}\text{U}$  per gram (the  $^{238}\text{U}$  concentration in the DOE-GJO U Standard) 609.3-keV gamma ray (energy just below the 661.6-keV  $^{137}\text{Cs}$  gamma-ray energy).

The average (dead-time-corrected) spectral peak intensities recorded for the base calibration of Gamma 2A were:

- C  $12.23 \pm 0.11$  counts per second for the 1460.8-keV gamma-ray peak, K Standard.
- C  $182.3 \pm 1.5$  counts per second for the 609.3-keV gamma-ray peak, U Standard.

The counting times for the base calibration measurements were 1,000 seconds per spectrum, but the examples will deal with a 100-second counting time per spectrum, which is the standard data acquisition time for field data. For a 100-second counting time, the number of counts in the 1460.8-keV spectral peak from the K Standard would be 1223 counts, and the 1s counting uncertainty would be 35.0 counts (the square root of 1223). Similarly, the number of counts in the 609.3-keV spectral

peak from the U Standard would be 18230, and the 1s counting uncertainty would be 135. Therefore, the two peak intensities for the Gamma 2A example will be

- C 12.23 ± 0.70 counts per second for the 1460.8-keV gamma-ray peak, K Standard.
- C 182.3 ± 2.7 counts per second for the 609.3-keV gamma-ray peak, U Standard.

The two uncertainties above are the 1s counting uncertainties divided by 100 seconds and doubled. The doubling makes the uncertainties consistent with MACTEC-ERS's use of 2s uncertainties in published results.

As explained in DOE (1995b), a gamma-ray source concentration is calculated with

$$concentration = \frac{27.027}{Y} I(E) \text{ (peak intensity)}, \quad (4-1)$$

in which  $Y$  is the gamma-ray yield, in gammas per decay, and 27.027 is a conversion factor, 27.027 picocuries = 1 decay per second.  $I(E)$  is the calibration function.

The gamma-ray yields published by Erdtmann and Soyka (1979) are

- C 0.107 gammas per decay for the 1460.8-keV gamma ray of  $^{40}\text{K}$ .
- C 0.461 gammas per decay for the 609.3-keV gamma ray of  $^{238}\text{U}$  (actually  $^{214}\text{Bi}$ ).

If  $sI$  is the uncertainty in  $I(E)$  and if  $sP$  is the uncertainty in the peak intensity  $P$ , then the uncertainty in the concentration is

$$(concentration) \sqrt{\left(\frac{sI}{I}\right)^2 + \left(\frac{sP}{P}\right)^2} \quad (4-2)$$

(assuming that the uncertainty in the yield  $Y$  is negligible).

Equations (1-2), (4-1), and (4-2) were used to calculate the concentrations and uncertainties associated with the two example spectral peak intensities (12.23 ± 0.70 counts per second for the 1460.8-keV gamma-ray peak, K Standard; 182.3 ± 2.7 counts per second for the 609.3-keV gamma-ray peak, U Standard) for the various  $C$  and  $D$  values from the different recalibrations. The concentrations are listed in the "Gamma 2A" part of Table 4-2.

The "Gamma 2B" part of Table 4-2 lists the analogous quantities for Gamma 2B. For Gamma 2B the two example peak intensities were

- C 14.13 ± 0.17 counts per second for the 1460.8-keV gamma-ray peak, SBK Standard.
- C 247.3 ± 2.2 counts per second for the 609.3-keV gamma-ray peak, SBU Standard.

These were the average intensities for spectra recorded by logging the SBK and SBT calibration standards, respectively, for the first calibration of Gamma 2B.

*Table 4-2. Illustrations of Logging System Efficiency Drifts*

	Calibration	$I(E)$ at $E = 1460.8 \text{ keV}$	$I(E)$ at $E = 609.3 \text{ keV}$	$^{40}\text{K}$ Concentration (pCi/g)	$^{238}\text{U}$ Concentration (pCi/g)
<b>Gamma 2A</b>	base	$0.0186 \pm 0.0023$	$0.0145 \pm 0.0019$	$57.6 \pm 7.8$	$155.5 \pm 20.4$
	recal 1	$0.0185 \pm 0.0035$	$0.0146 \pm 0.0029$	$57.1 \pm 11.3$	$155.8 \pm 31.2$
	recal 2	$0.0187 \pm 0.0035$	$0.0148 \pm 0.0029$	$57.9 \pm 11.4$	$158.2 \pm 31.6$
	recal 3	$0.0192 \pm 0.0034$	$0.0152 \pm 0.0028$	$59.2 \pm 11.0$	$162.7 \pm 30.3$
	recal 4	$0.0190 \pm 0.0014$	$0.0152 \pm 0.0012$	$58.6 \pm 5.6$	$162.6 \pm 13.1$
	recal 5	$0.0190 \pm 0.0015$	$0.0152 \pm 0.0012$	$58.7 \pm 5.7$	$162.4 \pm 13.5$
	recal 6	$0.0207 \pm 0.0023$	$0.0163 \pm 0.0019$	$63.9 \pm 7.9$	$174.2 \pm 20.3$
	recal 7	$0.0214 \pm 0.0022$	$0.0168 \pm 0.0018$	$66.0 \pm 7.7$	$180.1 \pm 19.6$
<b>Gamma 2B</b>	recal 4	$0.0159 \pm 0.0013$	$0.0132 \pm 0.0011$	$56.7 \pm 4.7$	$190.7 \pm 16.3$
	recal 5	$0.0161 \pm 0.0012$	$0.0134 \pm 0.0011$	$57.3 \pm 4.5$	$193.7 \pm 15.5$
	recal 6	$0.0165 \pm 0.0022$	$0.0135 \pm 0.0018$	$59.0 \pm 7.8$	$195.4 \pm 26.8$
	recal 7	$0.0168 \pm 0.0022$	$0.0137 \pm 0.0019$	$59.9 \pm 8.0$	$198.0 \pm 27.5$

The calculated  $^{40}\text{K}$  concentrations for Gamma 2A are plotted in relation to time in Figure 4-2.

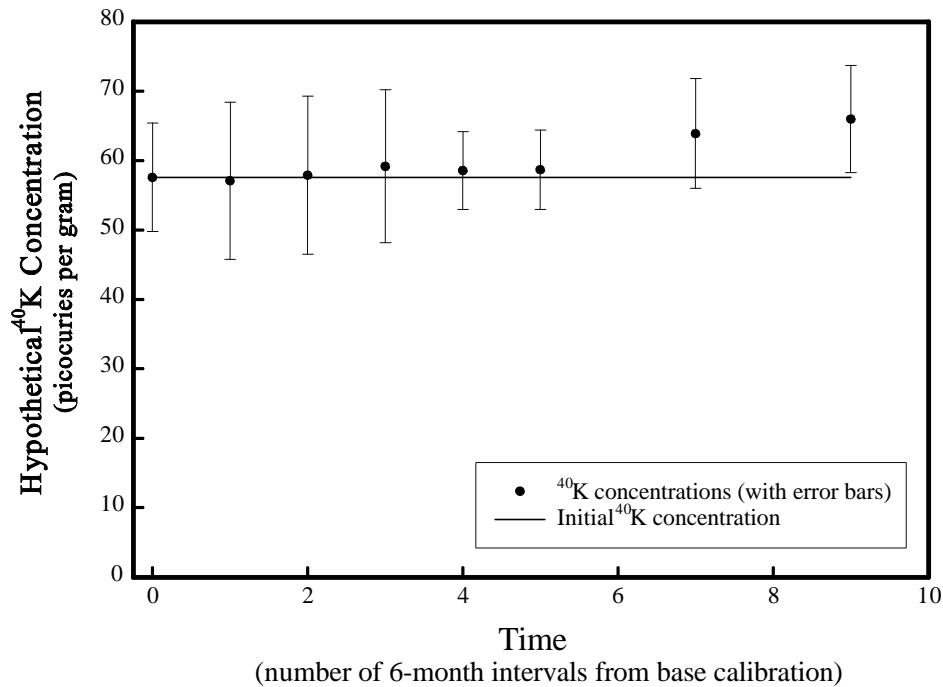


Figure 4-2. <sup>40</sup>K Concentrations Calculated Using a Fixed Peak Intensity ( $12.23 \pm 0.70$  counts per second, the average intensity from the K Model measurements for the base calibration) and the  $I(E)$  Values for the Various Calibrations

Figure 4-2 illustrates an effect of the decrease in logging system efficiency over time. The last two concentrations (i.e., the concentrations calculated with the  $I(E)$  for the sixth and seventh recalibrations) are offset from the other concentrations, but neither is identified as a data outlier if the set of concentrations depicted in the figure is analyzed with the Chauvenet criterion. Furthermore, each of the <sup>40</sup>K concentrations agrees, within the experimental uncertainties, with any other <sup>40</sup>K concentration in the set. Thus, the finding of all previous recalibrations remains valid. That is, a concentration derived from a spectral peak intensity using the  $I(E)$  from any particular calibration would agree, within uncertainties, with the concentration calculated using the  $I(E)$  from any other calibration.

At this point, the downward trend in logging system efficiency does not seem to indicate an incipient problem, but the efficiency should be monitored, perhaps by tracking the field verification spectra, to ensure early detection of any changes that might indicate electronic malfunctions.

## 5.0 New Field Verification Criteria

During field logging operations, field verification spectra are periodically acquired with the sonde outside of the borehole and with an Amersham *KUTh Field Verifier* (Amersham part number 188074) potassium-uranium-thorium gamma-ray source mounted on the sonde in a prescribed position relative to the detector. Field verifications serve as frequent confirmations of logging system efficiency and energy resolution. A system passes the efficiency check if the intensities of selected spectral peaks in the field verification spectra lie within acceptance limits. Likewise, the energy resolution is satisfactory if the FWHM of the selected spectral peaks fall within the acceptance limits. The peak intensity and FWHM limits, or tolerances, are updated at each recalibration.

Acceptance criteria are determined using control chart methods. Means and standard deviations ( $s$ ) are calculated for sets of data from all of the existing field verification spectra, and acceptance criteria are established in two levels: a *warning limit* is exceeded if a measurement deviates from the corresponding mean by  $2s$  to  $3s$ , and a *control limit* is exceeded if a measurement deviates from the mean by  $3s$  or more.

To implement these limits, a field verification spectrum is recorded and the FWHM and peak intensities are calculated for the spectral peaks associated with three gamma rays: 609.3 keV, 1460.8 keV, and 2614.5 keV. These FWHM and peak intensities are compared to the appropriate warning and control limits. The logging system passes or fails the acceptance test according to the outcomes listed in Tables 5-1 and 5-2.

*Table 5-1. Outcomes of Field Verification Measurements*

Test Result	Outcome
The FWHM and peak intensities for all three peaks lie within the warning limits.	The system passes the acceptance test.
One of the six FWHM and intensities exceeds the warning limits, but not the control limits.	Data from the next (follow-up) spectrum are examined. An outcome is determined from Table 5-2.
Two or more of the six FWHM and intensities exceed the warning limits.	The system fails the acceptance test.
One or more of the six FWHM and intensities exceeds the control limits.	The system fails the acceptance test.



*Table 5-2. Outcomes of Field Verification Measurements Involving Follow-up Spectra*

Test Result, Follow-up Spectrum	Outcome
The FWHM and peak intensities for all three peaks lie within the warning limits.	The system passes the acceptance test.
The FWHM or intensity that exceeded the warning limits, but not the control limits, in the earlier measurement now falls within the warning limits, but a different FWHM or intensity falls outside of the warning limits, but not the control limits.	Data from the next (third) spectrum are analyzed, and this table (5-2) is used to determine the outcome.
The FWHM or intensity that exceeded the warning limits, but not the control limits, in the earlier measurement exceeds the warning limits again, and lies on the same side of the data set mean as before.	The system fails the acceptance test.
The FWHM or intensity that exceeded the warning limits, but not the control limits, in the earlier measurement exceeds the warning limits again, but lies on the opposite side of the data set mean.	Data from the next (third) spectrum are analyzed. If the same FWHM or intensity falls outside of the warning limits again, the system fails the acceptance test.
Two or more of the six FWHM and intensities exceed the warning limits.	The system fails the acceptance test.
One or more of the six FWHM and intensities exceeds the control limits.	The system fails the acceptance test.

The project Technical Lead is notified of any acceptance test failure as soon as possible so that the cause of the failure can be determined and corrected.

Gamma 1A and Gamma 1B were not recalibrated in 1999, and only a few, if any, field verification spectra were recorded since the 1998 (sixth) recalibration. Therefore, new acceptance criteria were not established for these systems and the criteria from the sixth recalibration, reproduced in Tables 5-3 and 5-4, continue to be applicable.

*Table 5-3. Field Verification Acceptance Criteria for Gamma 1A<sup>1</sup>*

Gamma-Ray Energy (keV)	Parameter	Warning Limits		Control Limits	
		Lower	Upper	Lower	Upper
609.3	Peak intensity	8.86 c/s	10.07 c/s	8.56 c/s	10.37 c/s
	FWHM	1.82 KeV	2.52 KeV	1.65 KeV	2.69 KeV
1460.8	Peak intensity	9.83 c/s	11.24 c/s	9.48 c/s	11.59 c/s
	FWHM	2.18 KeV	2.76 KeV	2.04 KeV	2.90 KeV
2614.5	Peak intensity	2.12 c/s	2.51 c/s	2.02 c/s	2.61 c/s
	FWHM	2.59 KeV	3.36 KeV	2.40 KeV	3.55 KeV

<sup>1</sup> These criteria are applicable between January 23, 1998 and the establishment of new criteria at the next recalibration.

*Table 5-4. Field Verification Acceptance Criteria for Gamma 1B<sup>1</sup>*

Gamma-Ray Energy (keV)	Parameter	Warning Limits		Control Limits	
		Lower	Upper	Lower	Upper
<b>609.3</b>	Peak intensity	8.68 c/s	9.99 c/s	8.35 c/s	10.32 c/s
	FWHM	1.92 KeV	2.13 KeV	1.86 KeV	2.19 KeV
<b>1460.8</b>	Peak intensity	9.98 c/s	11.50 c/s	9.60 c/s	11.88 c/s
	FWHM	2.24 KeV	2.52 KeV	2.17 KeV	2.58 KeV
<b>2614.5</b>	Peak intensity	2.19 c/s	2.57 c/s	2.09 c/s	2.66 c/s
	FWHM	2.68 KeV	3.17 KeV	2.56 KeV	3.29 KeV

<sup>1</sup> These criteria are applicable between May 20, 1998 and the establishment of new criteria at the next recalibration.

For Gamma 2A, field verification criteria were established from statistical analysis of 968 field verification spectra collected prior to September 22, 1998. Warning and control limits for Gamma 2A are shown in Table 1-3 in Section 1.3. These acceptance criteria are applicable until new acceptance criteria are established at the next recalibration.

For Gamma 2B, field verification criteria were established from statistical analysis of 471 field verification spectra collected prior to December 10, 1999. Warning and control limits for Gamma 2B are shown in Table 1-4 in Section 1.3. These acceptance criteria are applicable until new acceptance criteria are established at the next recalibration.

## **6.0 Acknowledgments**

R.G. McCain analyzed the field verification spectra and determined the field verification criteria.

R.M. Paxton transformed a disorganized set of text, figures, and tables into the finished report.

R.A. Showalter proposed that the large uncertainties in the generalized corrections for casing and water in the borehole would be reduced if the corrections were derived by certain curve fitting or linear interpolation methods. The derivations are described in Appendix A and Appendix B.

## 7.0 References

Erdtmann, G., and W. Soyka, 1979. *The Gamma Rays of the Radionuclides*, Verlag Chemie, New York.

Friedlander, G., J.W. Kennedy, E.S. Macias, and J.M. Miller, 1981. *Nuclear and Radiochemistry* (Third Edition), John Wiley and Sons, Inc., New York.

Heistand, B.E., and E.F. Novak, 1984. *Parameter Assignments for Spectral Gamma-Ray Borehole Calibration Models*, GJBX-(284), prepared by Bendix Field Engineering Corporation for the U.S. Department of Energy Grand Junction Projects Office, Grand Junction, Colorado.

Leino, R., D.C. George, B.N. Key, L. Knight, and W.D. Steele, 1994. *Field Calibration Facilities for Environmental Measurement of Radium, Thorium, and Potassium*, DOE/ID/12584-179 GJ/TMC-01 (Third Edition) UC-902, prepared by RUST Geotech, Inc., for the U.S. Department of Energy Grand Junction Office, Grand Junction, Colorado.

Taylor, J.R., 1982. *An Introduction to Error Analysis*, University Science Books, Mill Valley, California.

Trahey, N.M., A.M. Voeks, and M.D. Soriano, 1982. *Grand Junction/New Brunswick Laboratory Interlaboratory Measurement Program: Part I -- Evaluation; Part II -- Methods Manual*, Report NBL-303, New Brunswick Laboratory, Argonne, Illinois.

U.S. Department of Energy, 1995a. *Vadose Zone Monitoring Project at the Hanford Tank Farms Spectral Gamma-Ray Borehole Geophysical Logging Characterization and Baseline Monitoring Plan for the Hanford Single-Shell Tanks* (Rev. 0), P-GJPO-1786, prepared by Rust Geotech for the U.S. Department of Energy Grand Junction Office, Grand Junction, Colorado.

\_\_\_\_\_, 1995b. *Vadose Zone Monitoring Project at the Hanford Tank Farms Calibration of Two Spectral Gamma-Ray Logging Systems for Baseline Characterization Measurements in the Hanford Tank Farms* (Rev. 0), GJPO-HAN-1, prepared by Rust Geotech for the U.S. Department of Energy Grand Junction Office, Grand Junction, Colorado.

\_\_\_\_\_, 1996a. *Vadose Zone Characterization Project at the Hanford Tank Farms, Biannual Recalibration of Two Spectral Gamma-Ray Logging Systems Used for Baseline Characterization Measurements in the Hanford Tank Farms* (Rev. 0), DOE/ID/12584-266 GJPO-HAN-3, prepared by Rust Geotech for the U.S. Department of Energy Grand Junction Office, Grand Junction, Colorado.

U.S. Department of Energy, 1996b. *Vadose Zone Characterization Project at the Hanford Tank Farms, Second Biannual Recalibration of Two Spectral Gamma-Ray Logging Systems Used for Baseline Characterization Measurements in the Hanford Tank Farms* (Rev. 0), DOE/ID/12584-281 GJPO-HAN-5, prepared by Rust Geotech for the U.S. Department of Energy Grand Junction Office, Grand Junction, Colorado.

\_\_\_\_\_, 1997. *Hanford Tank Farms Vadose Zone, Third Biannual Recalibration of Two Spectral Gamma-Ray Logging Systems Used for Baseline Characterization Measurements in the Hanford Tank Farms* (Rev. 0), GJO-97-22-TAR GJO-HAN-13, prepared by MACTEC-ERS for the U.S. Department of Energy Grand Junction Office, Grand Junction, Colorado.

\_\_\_\_\_, 1998a. *Hanford Tank Farms Vadose Zone, Fourth Biannual Recalibration of Spectral Gamma-Ray Logging Systems Used for Baseline Characterization Measurements in the Hanford Tank Farms* (Rev. 0), GJO-97-23-TAR GJO-HAN-14, prepared by MACTEC-ERS for the U.S. Department of Energy Grand Junction Office, Grand Junction, Colorado.

\_\_\_\_\_, 1998b. *Hanford Tank Farms Vadose Zone, Fifth Biannual Recalibration of Spectral Gamma-Ray Logging Systems Used for Baseline Characterization Measurements in the Hanford Tank Farms* (Rev. 0), GJO-98-41-TAR GJO-HAN-20, prepared by MACTEC-ERS for the U.S. Department of Energy Grand Junction Office, Grand Junction, Colorado.

\_\_\_\_\_, 1999. *Hanford Tank Farms Vadose Zone, Sixth Biannual Recalibration of Spectral Gamma-Ray Logging Systems Used for Baseline Characterization Measurements in the Hanford Tank Farms* (Rev. 0), GJO-99-100-TAR GJO-HAN-26, prepared by MACTEC-ERS for the U.S. Department of Energy Grand Junction Office, Grand Junction, Colorado.

# **Appendix A**

## **Updated General Corrections for Borehole Casing**

# A1.0 Updated General Corrections for Borehole Casing

## A1.1 Background

A casing correction for a particular thickness of steel casing and a particular gamma-ray energy  $E$  is defined as

$$K = K(E) = \frac{\text{intensity of the spectral peak recorded without casing}}{\text{intensity of the spectral peak recorded with casing}}. \quad (\text{A1-1})$$

“Spectral peak” refers to the full energy peak in a spectrum corresponding to a discrete gamma-ray energy  $E$ . Because the casing attenuation depends on  $E$ , the correction for a particular casing thickness is a function of  $E$ .

For the base SGLS calibrations (DOE 1995b), casing correction data were collected by logging the DOE-GJO KW Model (Leino et al. 1994) with and without pieces of steel test casing in the test hole. Four sections of test casing, with wall thicknesses of 0.25 inches, 0.33 inches, 0.375 inches, and 0.65 inches were available for measurements, so spectra were recorded with each of the four thicknesses, and in addition, with a thickness of 0.98 inches that was created by placing the 0.33-inch casing within the 0.65-inch casing. The large diameter test holes (7.0-inch, 9.0-inch, and 12.0-inch diameters) in the KW Model accommodated the test casings, and the model’s potassium, uranium, and thorium sources endowed the spectra with numerous peaks. The peak intensities were determined, then Equation (A1-1) was used to calculate correction values for the many discrete gamma-ray energies and the five thicknesses.

If the corrections for any particular casing thickness were plotted in relation to  $E$ , the pattern established by the data points indicated that the corrections were related to the energies by simple analytical functions. Using the *TableCurve* program to curve-fit the data over the variable  $E$ , a suitable function for each thickness was determined so that corrections for energies not represented in the calibration standards, such as 661.6 keV ( $^{137}\text{Cs}$ ), could be calculated. The curve fitting indicated that the equation presented in the base calibration report (DOE 1995b),

$$K(E) = \frac{1}{A_C \% \frac{B_C}{\ln(E)}}, \quad (\text{A1-2})$$

closely simulated the relationship between correction and gamma-ray energy. The parameters  $A_C$  and  $B_C$  assumed values that were specific to the casing thickness. The values for the five casing thicknesses used in the measurements are listed in Tables 8-1 and 8-2 in the base calibration report, and are replicated in Tables A1-2 and A1-3 in this report.

The application of the casing correction is indicated by Equation (A1-1). If a spectrum is recorded by logging a cased borehole, the intensity of a peak in that spectrum can be multiplied by  $K(E)$  (calculated with the appropriate  $A_C$ ,  $B_C$ , and  $E$ ) to determine the peak intensity that would have been recorded if the borehole had not been cased.

Equation (A1-2) and the  $A_C$  and  $B_C$  values in Tables 8-1 and 8-2 in DOE (1995b) would have provided all of the required casing corrections if the thicknesses of the casings in the boreholes at Hanford had been equal to the thicknesses of the test casings used for casing correction measurements. But unfortunately, none of the casing thicknesses encountered at Hanford have matched any of the five casing thicknesses. The most common casing thickness in the Hanford boreholes is 0.280 inches (6-inch-diameter casing); other observed thicknesses are 0.237 inches (4-inch-diameter), 0.322 inches (8-inch-diameter), and 0.365 inches (10-inch-diameter).

A general analysis of the casing corrections is described in the third biannual recalibration report (DOE 1997). For this analysis, the casing corrections derived from the measurements were analyzed as functions of casing thickness for particular energies, instead of as functions of energy for particular thicknesses. Curve-fitting with casing thickness as the variable (as opposed to curve-fitting with gamma-ray energy as the variable) showed that all of the correction-versus-casing-thickness data could be simulated by the equation

$$K = \exp(F + GT^3 + HT^4), \quad (\text{A1-3})$$

in which  $T$  is the casing thickness, in inches, and  $F$ ,  $G$ , and  $H$  are curve fitting parameters. Further analysis indicated that  $F$ ,  $G$ , and  $H$  could be expressed as functions that depend on the gamma-ray energy (see Equations (4-3), (4-4), and (4-5), and Figures 4-2, 4-3, and 4-4 in DOE 1997).

The equations for  $K$  and  $F$ ,  $G$ , and  $H$  could be used to calculate the casing correction for any gamma-ray energy between 186 keV and 2614 keV and any thickness of steel casing between 0 and 1.0 inch. However, Figures 4-2, 4-3, and 4-4 in DOE (1997) show that  $F$ ,  $G$ , and  $H$  have large relative uncertainties. Thus, though the method is technically correct, it yields corrections with large relative uncertainties. Large relative uncertainties in the corrections lead to calculated radionuclide concentrations with large “error bars.” This is a disadvantage to monitoring because small but real changes in concentration could be masked by large error bars on the concentrations calculated from the original and repeat log data.

## **A1.2 Corrections Reformulated to Reduce Uncertainties**

### **A1.2.1 Linear Interpolation for $F$ , $G$ , and $H$**

Because parts of the relative uncertainties in  $F$ ,  $G$ , and  $H$  originated in curve fitting, the possibility of reducing the uncertainties by eliminating the curve fitting was explored. That is, instead of using Equations (4-3), (4-4), and (4-5) in DOE (1997) to calculate values for  $F$ ,  $G$ , and  $H$  at some energy



$E$ , each desired value would be calculated by linear interpolation between two energies  $E_1$  and  $E_2$  (with  $E_1 < E < E_2$ ), where  $E_1$  and  $E_2$  are energies for which values of  $F$ ,  $G$ , and  $H$  were determined by the curve fitting that led to Equation (A1-3) (see Tables 4-1 and 4-2 in DOE 1997).

The corrections displayed in Table A1-1 were all calculated with Equation (A1-3), but the “general casing correction” values were calculated with values of  $F$ ,  $G$ , and  $H$  derived from Equations (4-3), (4-4), and (4-5) in DOE (1997), whereas the “2-point interpolation correction” values were calculated with values of  $F$ ,  $G$ , and  $H$  derived from 2-point interpolations between energies. It is apparent that the two sets of corrections are in good agreement, that the corrections calculated by the general method have large uncertainties, and that the corrections calculated with interpolated values of  $F$ ,  $G$ , and  $H$  are generally smaller, but only marginally so.

*Table A1-1. Examples of Casing Corrections Calculated by the General Method and the Method Based on 2-Point Linear Interpolation of  $F$ ,  $G$ , and  $H$*

Casing Thickness (inches)	Gamma-Ray Energy (keV)	Gamma 1		Gamma 2	
		General Casing Correction	2-Point Interpolation Correction	General Casing Correction	2-Point Interpolation Correction
0.280	609.3 ( $^{226}\text{Ra}$ )	$1.68 \pm 0.48$	$1.68 \pm 0.43$	$1.57 \pm 0.63$	$1.58 \pm 0.70$
	661.6 ( $^{137}\text{Cs}$ )	$1.65 \pm 0.46$	$1.66 \pm 0.38$	$1.54 \pm 0.60$	$1.57 \pm 0.33$
	1173.2 ( $^{60}\text{Co}$ )	$1.46 \pm 0.35$	$1.47 \pm 0.22$	$1.39 \pm 0.43$	$1.39 \pm 0.27$
	1332.5 ( $^{60}\text{Co}$ )	$1.43 \pm 0.34$	$1.45 \pm 0.18$	$1.36 \pm 0.40$	$1.38 \pm 0.17$
	1460.8 ( $^{40}\text{K}$ )	$1.41 \pm 0.33$	$1.42 \pm 0.18$	$1.35 \pm 0.38$	$1.36 \pm 0.18$
	1764.5 ( $^{226}\text{Ra}$ )	$1.37 \pm 0.31$	$1.38 \pm 0.17$	$1.31 \pm 0.35$	$1.34 \pm 0.12$
	2614.5 ( $^{232}\text{Th}$ )	$1.30 \pm 0.29$	$1.31 \pm 0.23$	$1.25 \pm 0.29$	$1.25 \pm 0.18$
0.322	609.3 ( $^{226}\text{Ra}$ )	$1.81 \pm 0.54$	$2.24 \pm 0.69$	$1.68 \pm 0.69$	$1.69 \pm 0.76$
	661.6 ( $^{137}\text{Cs}$ )	$1.77 \pm 0.51$	$1.78 \pm 0.42$	$1.64 \pm 0.66$	$1.67 \pm 0.36$
	1173.2 ( $^{60}\text{Co}$ )	$1.55 \pm 0.38$	$1.56 \pm 0.23$	$1.46 \pm 0.47$	$1.46 \pm 0.29$
	1332.5 ( $^{60}\text{Co}$ )	$1.51 \pm 0.36$	$1.53 \pm 0.19$	$1.43 \pm 0.44$	$1.45 \pm 0.18$
	1460.8 ( $^{40}\text{K}$ )	$1.48 \pm 0.35$	$1.50 \pm 0.19$	$1.41 \pm 0.42$	$1.42 \pm 0.19$
	1764.5 ( $^{226}\text{Ra}$ )	$1.44 \pm 0.33$	$1.45 \pm 0.18$	$1.36 \pm 0.38$	$1.39 \pm 0.13$
	2614.5 ( $^{232}\text{Th}$ )	$1.35 \pm 0.31$	$1.36 \pm 0.25$	$1.29 \pm 0.31$	$1.29 \pm 0.18$

## A1.2.2 Curve Fitting for $A_C$ and $B_C$

Because 2-point linear interpolation of  $F$ ,  $G$ , and  $H$  did not yield significant reductions in the correction uncertainties, a different method was tried. This method started with the basic correction equation, Equation (A1-2). The values of  $A_C$  and  $B_C$  in Equation (A1-2) depend on the casing thickness  $T$ , and particular values for the two parameters had been determined for five different casing thicknesses. Curve fitting was applied to find functions that simulated the relationships between  $A_C$  and  $T$  and  $B_C$  and  $T$ . These functions were then used to calculate values for  $A_C$  and  $B_C$  for selected casing thicknesses.

Parameter  $B_C$  is considered first.

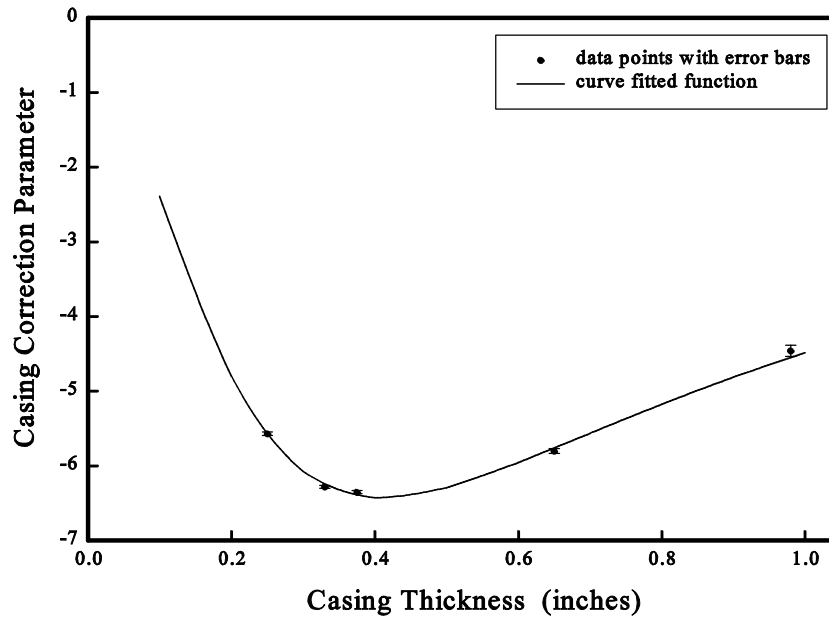


Figure A1-1. Casing Correction Parameter  $B_C$  Plotted in Relation to Casing Thickness

Symbols in Figure A1-1 show the five values of parameter  $B_C$ , with error bars, that were determined from base calibration measurements using the five test casings. Analysis of these data with the curve fitting program indicated that a good fit is provided by the function

$$B_C = \frac{1}{U + V\sqrt{T} + \frac{W\ln(T)}{T}} \quad (\text{A1-4})$$

In Equation (A1-4),  $T$  is the casing wall thickness, in inches, and  $U$ ,  $V$ , and  $W$  are curve fitting constants with values as follows:

$$U = 0.053 \pm 0.014$$

$$V = -0.170 \pm 0.022$$

$$W = 0.0151 \pm 0.0019.$$

The curve in the plot of Figure A1-1 depicts the relationship between  $B_C$  and  $T$  specified by Equation (A1-4).

Several other equations provided as good a fit to the data as Equation (A1-4), but Equation (A1-4) was selected on the basis of its property that  $B_C$  will approach zero if  $T$  approaches zero. This was considered desirable behavior because the correction  $K(E)$  calculated with Equation (A1-2) should be independent of  $E$  and should be equal to 1 if the casing thickness  $T$  is zero.  $K(E)$  will have the desired behavior if  $B_C \neq 0$  and  $A_C \neq 1$  when  $T \neq 0$ .

Application of the standard propagation of uncertainties theorem (Taylor 1982) to Equation (A1-4) indicates that the uncertainty in  $B_C$  is

$$s B_C = \left( B_C^2 \right)^{1/2} \sqrt{(s U)^2 + (T \otimes V)^2 + \left( \frac{\ln(T)}{T} \otimes W \right)^2}. \quad (\text{A1-5})$$

Uncertainties calculated with Equation (A1-5) are not unduly large.

Unfortunately, the situation with the  $A_C$  parameter in Equation (A1-2) is not so straightforward.

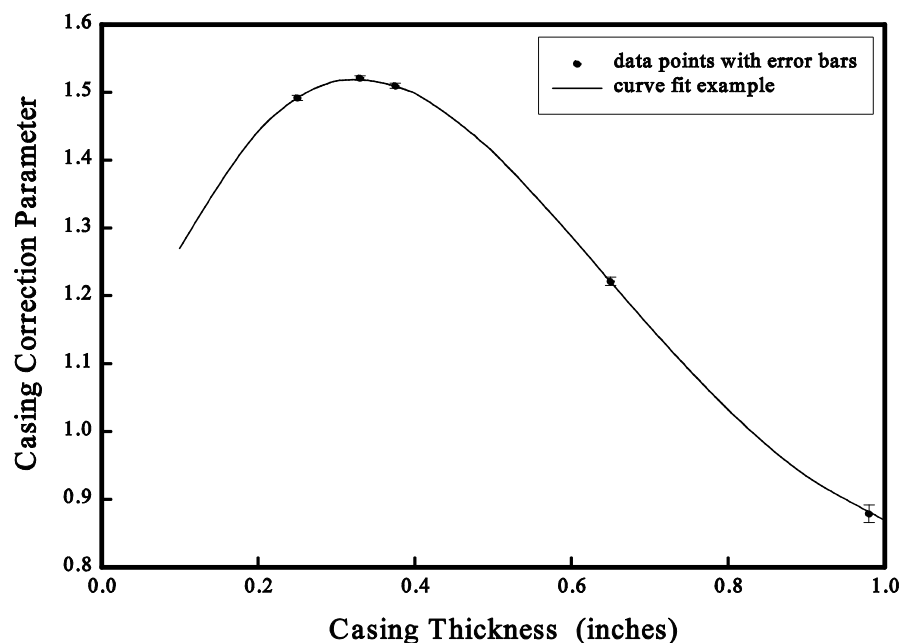


Figure A1-2. Casing Correction Parameter  $A_C$  Plotted in Relation to Casing Thickness

Symbols in Figure A1-2 represent values for the casing correction parameter  $A_C$  in relation to the casing thickness, as determined from the base calibration measurements using the five test casings.

Curve fitting indicated that a number of functions could accurately simulate the relationship between  $A_C$  and the casing thickness. Two functions were selected on the basis that they predicted values close to  $A_C = 1$  when the thickness approached zero. This was considered a desirable trait because, as mentioned previously, the correction calculated with Equation (A1-2) should approach one as the casing thickness approaches zero. (That is,  $K(E) \approx 1$  when  $T \approx 0$  if  $B_C \approx 0$  and  $A_C \approx 1$  when  $T \approx 0$ .)

One function is

$$A_C = L + MT + NT^2 + Pe^{PT}. \quad (\text{A1-6})$$

The curve fitting constants are

$$L = -13.2 \pm 8.5$$

$$M = -10.5 \pm 6.4$$

$$N = -13.9 \pm 7.4$$

$$P = 14.2 \pm 8.2.$$

The uncertainty of  $A_C$  is

$$sA_C = \sqrt{(sL)^2 + (T sM)^2 + (T^2 sN)^2 + (e^{PT} sP)^2}. \quad (\text{A1-7})$$

If the uncertainties in the curve fitting constants are entered in Equation (A1-7), the result,

$$sA_C = \sqrt{(8.5)^2 + (6.4T)^2 + (7.4T^2)^2 + (8.2e^T)^2}, \quad (\text{A1-8})$$

points to the obvious problem that  $sA_C$  will have a large value for any value of  $T$ . This is illustrated by the values for  $A_C$ ,  $sA_C$ ,  $B_C$ , and  $sB_C$  that were calculated with Equations (A1-6), (A1-8), (A1-4), and (A1-5) for the 0.28-inch-thick casing:

$$A_C = 1.5 \pm 13.9$$

$$B_C = -5.91 \pm 0.61.$$

The large uncertainty in  $A_C$  produces, not surprisingly, a large uncertainty in the casing correction  $K(E)$  when  $K(E)$  is calculated using these  $A_C$  and  $B_C$  values and Equation (A1-2). For example,  $K(E) = 1.7 \pm 38.4$  for the casing thickness of 0.28 inches and the gamma-ray energy 661.6 keV.

Another equation deduced by curve fitting is

$$A_C = \exp(L + MT + NT^2 + PT^3). \quad (\text{A1-9})$$

The curve in Figure A1-2 is a plot of  $A_C$  in relation to  $T$  determined by Equation (A1-9). Values for  $A_C$  calculated with Equation (A1-9) have smaller uncertainties, for example,  $A_C = 1.51 \pm 0.15$  for the 0.28-inch-thick casing. The uncertainty in the correction  $K(E)$  is correspondingly smaller, but is still

about as large as the uncertainty resulting from use of the general casing correction equations. For example, for the thickness of 0.28 inches and the gamma-ray energy 661.6 keV,  $K(E) = 1.67 \pm 0.49$ .

### A1.3 The Recommended Method: Linear Interpolation for $A_C$ and $B_C$

The disappointing results from the curve fittings prompted evaluation of a different method. This method is based on the observation that the data displayed in Figures A1-1 and A1-2 imply that both  $A_C$  and  $B_C$  are related to the casing thickness by functions that are slowly varying and are free of cusps, singularities, multiple oscillations, and other pathological features. Then to a good approximation,  $A_C$  and  $B_C$  are linear in relation to casing thickness between any two sequential data points. This implies that values for  $A_C$  and  $B_C$  for arbitrary thicknesses can be calculated by linear interpolation. In particular, if values were established for  $A_C$  and  $B_C$  by measurements for two particular casing thicknesses  $T_1$  and  $T_2$ , then the values for  $A_C$  and  $B_C$  for an intermediate thickness  $T$  ( $T_1 < T < T_2$ ) can be calculated as follows.

If  $A_1$  and  $A_2$  are the  $A_C$  values for the casing thicknesses  $T_1$  and  $T_2$ , respectively, and if  $B_1$  and  $B_2$  are the  $B_C$  values for the same thicknesses, then linear interpolation indicates that the  $A_C$  and  $B_C$  values for the intermediate thickness  $T$  ( $T_1 < T < T_2$ ) are:

$$A_C = \left( 1 + \frac{T - T_1}{T_2 - T_1} \right) A_1 + \left( \frac{T - T_1}{T_2 - T_1} \right) A_2 \quad (\text{A1-10})$$

and

$$B_C = \left( 1 + \frac{T - T_1}{T_2 - T_1} \right) B_1 + \left( \frac{T - T_1}{T_2 - T_1} \right) B_2. \quad (\text{A1-11})$$

The associated uncertainties are

$$sA_C = \sqrt{\left( 1 + \frac{T - T_1}{T_2 - T_1} \right)^2 (sA_1)^2 + \left( \frac{T - T_1}{T_2 - T_1} \right)^2 (sA_2)^2} \quad (\text{A1-12})$$

and

$$sB_C = \sqrt{\left( 1 + \frac{T - T_1}{T_2 - T_1} \right)^2 (sB_1)^2 + \left( \frac{T - T_1}{T_2 - T_1} \right)^2 (sB_2)^2}. \quad (\text{A1-13})$$

The Gamma 1A values for  $A_C$ ,  $sA_C$ ,  $B_C$ , and  $sB_C$  for the five casing thicknesses were listed in Table 8-1 in the base calibration report (DOE 1995b), and are replicated in Table A1-2.

*Table A1-2. Casing Correction Parameters for Gamma 1A*

Casing Thickness (inches)	$A_C$	$B_C$
0.25	$1.492 \pm 0.0038$	$-5.571 \pm 0.023$
0.33	$1.5213 \pm 0.0031$	$-6.283 \pm 0.018$
0.375	$1.5098 \pm 0.0037$	$-6.355 \pm 0.022$
0.65	$1.2214 \pm 0.0061$	$-5.802 \pm 0.034$
0.98	$0.879 \pm 0.013$	$-4.460 \pm 0.074$

Likewise, the Gamma 2A values for  $A_C$ ,  $sA_C$ ,  $B_C$ , and  $sB_C$  for the five casing thicknesses were listed in Table 8-2 in the base calibration report (DOE 1995b), and are replicated in Table A1-3.

*Table A1-3. Casing Correction Parameters for Gamma 2A*

Casing Thickness (inches)	$A_C$	$B_C$
0.25	$1.5148 \pm 0.0080$	$-5.768 \pm 0.048$
0.33	$1.4628 \pm 0.0049$	$-5.928 \pm 0.029$
0.375	$1.4777 \pm 0.0050$	$-6.179 \pm 0.029$
0.65	$1.2051 \pm 0.0061$	$-5.711 \pm 0.034$
0.98	$0.836 \pm 0.014$	$-4.206 \pm 0.078$

The  $A_C$  and  $B_C$  values for the casing thickness of 0.280 inches, for example, would be calculated with Equations (A1-10) and (A1-11) and the following thicknesses (for both Gamma 1A and Gamma 2A):

$$T = 0.28 \text{ inches}$$

$$T_1 = 0.25 \text{ inches}$$

$$T_2 = 0.33 \text{ inches.}$$

For Gamma 1A, the  $A_1$ ,  $A_2$ ,  $B_1$ , and  $B_2$  values would be

$$A_1 = 1.492$$

$$A_2 = 1.5213$$

$$B_1 = -5.571$$

$$B_2 = -6.283,$$

and for Gamma 2A the values would be

$$A_1 = 1.5148$$

$$A_2 = 1.4628$$

$$B_1 = -5.768$$

$$B_2 = -5.928.$$

Table A1-4 displays some representative corrections calculated by the linear interpolation method, and for comparison, the corresponding corrections calculated with the generalized method described in the third biannual recalibration report (DOE 1997).

*Table A1-4. Casing Corrections: Interpolated Corrections Versus General Corrections*

Casing Thickness (inches)	Gamma-Ray Energy (keV)	Gamma 1		Gamma 2	
		Interpolated Correction	General Correction	Interpolated Correction	General Correction
0.280	186.0	$2.592 \pm 0.027$	$2.62 \pm 1.15$	$2.631 \pm 0.056$	$2.47 \pm 1.55$
	609.0	$1.688 \pm 0.010$	$1.68 \pm 0.48$	$1.705 \pm 0.021$	$1.57 \pm 0.63$
	662.0	$1.655 \pm 0.010$	$1.65 \pm 0.46$	$1.672 \pm 0.020$	$1.54 \pm 0.59$
	1173.0	$1.477 \pm 0.008$	$1.46 \pm 0.35$	$1.491 \pm 0.016$	$1.39 \pm 0.43$
	1333.0	$1.446 \pm 0.007$	$1.43 \pm 0.34$	$1.459 \pm 0.015$	$1.36 \pm 0.40$
	1461.0	$1.425 \pm 0.007$	$1.41 \pm 0.33$	$1.438 \pm 0.014$	$1.35 \pm 0.38$
	1764.0	$1.385 \pm 0.007$	$1.37 \pm 0.31$	$1.397 \pm 0.013$	$1.31 \pm 0.35$
	2615.0	$1.314 \pm 0.006$	$1.30 \pm 0.29$	$1.325 \pm 0.012$	$1.25 \pm 0.29$
0.322	186.0	$3.033 \pm 0.039$	$2.98 \pm 1.36$	$2.970 \pm 0.060$	$2.78 \pm 1.81$
	609.0	$1.820 \pm 0.013$	$1.81 \pm 0.54$	$1.832 \pm 0.020$	$1.68 \pm 0.69$
	662.0	$1.779 \pm 0.012$	$1.77 \pm 0.51$	$1.793 \pm 0.019$	$1.64 \pm 0.66$
	1173.0	$1.564 \pm 0.009$	$1.55 \pm 0.38$	$1.584 \pm 0.015$	$1.46 \pm 0.47$
	1333.0	$1.527 \pm 0.008$	$1.51 \pm 0.36$	$1.547 \pm 0.014$	$1.43 \pm 0.44$
	1461.0	$1.502 \pm 0.008$	$1.48 \pm 0.35$	$1.523 \pm 0.013$	$1.41 \pm 0.42$
	1764.0	$1.455 \pm 0.008$	$1.44 \pm 0.33$	$1.477 \pm 0.012$	$1.36 \pm 0.38$
	2615.0	$1.372 \pm 0.007$	$1.35 \pm 0.31$	$1.395 \pm 0.011$	$1.29 \pm 0.31$
0.365	186.0	$3.341 \pm 0.050$	$3.41 \pm 1.61$	$3.304 \pm 0.066$	$3.13 \pm 2.12$
	609.0	$1.909 \pm 0.015$	$1.95 \pm 0.60$	$1.925 \pm 0.020$	$1.80 \pm 0.77$
	662.0	$1.864 \pm 0.014$	$1.90 \pm 0.57$	$1.881 \pm 0.019$	$1.75 \pm 0.73$
	1173.0	$1.625 \pm 0.010$	$1.64 \pm 0.42$	$1.645 \pm 0.014$	$1.53 \pm 0.51$
	1333.0	$1.584 \pm 0.010$	$1.59 \pm 0.40$	$1.604 \pm 0.013$	$1.50 \pm 0.48$
	1461.0	$1.557 \pm 0.009$	$1.56 \pm 0.38$	$1.577 \pm 0.013$	$1.47 \pm 0.45$
	1764.0	$1.505 \pm 0.009$	$1.51 \pm 0.36$	$1.526 \pm 0.012$	$1.42 \pm 0.41$
	2615.0	$1.415 \pm 0.007$	$1.41 \pm 0.33$	$1.436 \pm 0.010$	$1.33 \pm 0.33$

The linear interpolation yields corrections that agree (within uncertainties) with the corrections calculated by the generalized method, but the uncertainties associated with the linear interpolation are much smaller than the uncertainties associated with the generalized method. Therefore, the replacement of the generalized method with the linear interpolation method can be recommended. The minor drawback is that the values of the  $A_C$  and  $B_C$  parameters in Equation (A1-2) will have to be manually calculated for each casing thickness.

## A1.4 Summary

The recommended method was used to calculate  $A_C$  and  $B_C$  values for three of the four most common casing thicknesses at Hanford. These values are presented in Table A1-5 for Gamma 1A, and in Table A1-6 for Gamma 2A.

The  $A_C$  and  $B_C$  values for the 0.237-inch-thick casing (4.0-inch diameter) could not be calculated by linear interpolation because the thickness is smaller than 0.25 inches, which is the smallest thickness used for measurements. Estimates for the  $A_C$  and  $B_C$  values for 0.237-inch-thick casing could, however, be gained by linear *extrapolation*. Although extrapolation should generally be used with caution, it can be defended in the present case because the 0.237-inch thickness lies fairly close to the thickness of 0.25 inches for which measurements were made. It should be noted that in the thickness range from  $T = 0.237$  inches to  $T = 0.25$  inches, the curve fit function for  $A_C$  (Figure A1-2) has a greater curvature than the curve fit function for  $B_C$  (Figure A1-1). This indicates that linear extrapolation is more likely to yield an inaccurate value for  $A_C$  than for  $B_C$ .

*Table A1-5. Casing Correction Parameters for Gamma 1A*

Casing Thickness (inches)	$A_C$	$B_C$
0.237	$1.4872 \pm 0.0044$	$-5.455 \pm 0.027$
0.280	$1.5030 \pm 0.0026$	$-5.838 \pm 0.016$
0.322	$1.5184 \pm 0.0028$	$-6.212 \pm 0.016$
0.365	$1.5124 \pm 0.0030$	$-6.339 \pm 0.018$

*Table A1-6. Casing Correction Parameters for Gamma 2A*

Casing Thickness (inches)	$A_C$	$B_C$
0.237	$1.5233 \pm 0.0093$	$-5.742 \pm 0.056$
0.280	$1.4953 \pm 0.0053$	$-5.828 \pm 0.032$
0.322	$1.4680 \pm 0.0045$	$-5.912 \pm 0.027$
0.365	$1.4744 \pm 0.0040$	$-6.123 \pm 0.023$

The values for  $A_C$  and  $B_C$  in Tables A1-5 and A1-6 have been installed in the project's data analysis software. Thus, casing corrections for the four thicknesses can be calculated and used to correct spectral peak intensities by executing the analysis software in the usual way.

For the seventh recalibration, data were collected to demonstrate the accuracy of the corrections predicted by the interpolated  $A_C$  and  $B_C$  values for the 0.280-inch-thick casing. Spectra were recorded by logging the calibration standards SBU, SBT, and SBM in the usual (open hole) way, and in addition, the three standards were logged with the Gamma 2A sonde enclosed by a recently acquired



0.280-inch-thick section of test casing. The intensities of full energy peaks in all of the spectra were calculated. For each gamma-ray energy, the average intensity from the open hole spectra from a particular calibration standard was determined, and likewise the average intensity from the cased hole spectra was determined. Then, for each energy the correction was calculated using the average intensities and Equation (A1-1); the symbols with error bars in the graph of Figure A1-3 represent these corrections.

The curve in Figure A1-3 represents the corrections calculated with Equation (A1-2) and the values of  $A_C$  and  $B_C$  in Table A1-6 for the 0.280-inch-thick casing.

The measured corrections are obviously in excellent agreement with the corrections predicted by Equation (A1-2) and the values of  $A_C$  and  $B_C$  derived by linear interpolation.

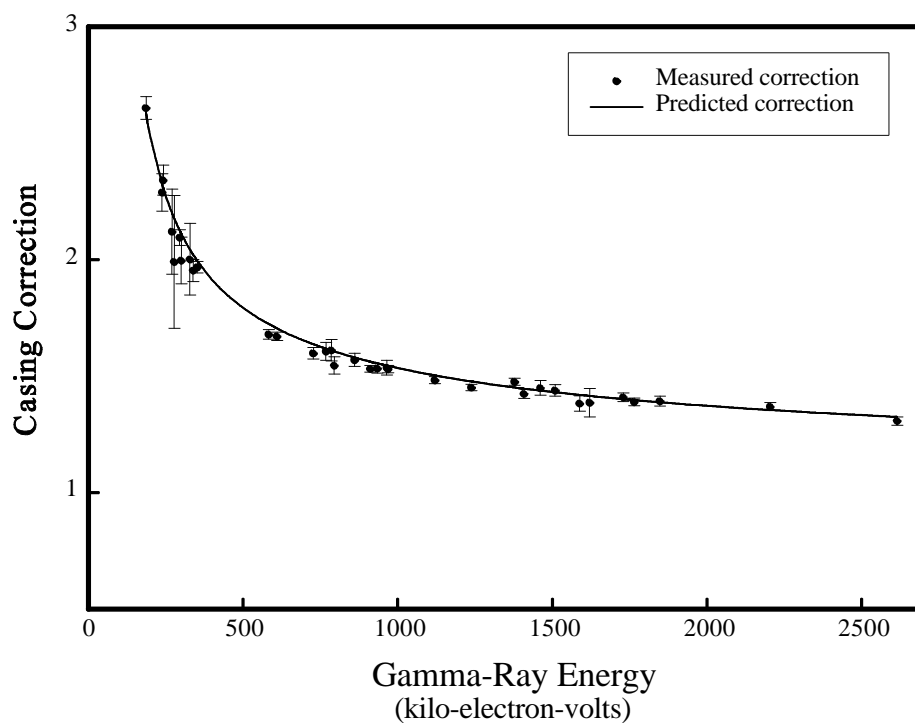


*Figure A1-3. Predicted Casing Corrections for the 0.280-inch-thick Casing Compared to the Measured Corrections*

## **Appendix B**

# **Updated General Corrections for Water-Filled Boreholes**

# B1.0 Updated General Corrections for Water-Filled Boreholes

## B1.1 Background

The SGLS calibrations were formulated for analysis of data from uncased boreholes with no liquid. Log data recorded with the sonde immersed in water must therefore be corrected for the attenuation of gamma rays by the water before the gamma-ray source concentrations are calculated. For a particular borehole diameter, the correction depends on the gamma-ray energy  $E$  and is defined as

$$\text{correction} = K(E) = \frac{\text{intensity of peak from dry borehole log}}{\text{intensity of peak from water\&filled borehole log}}. \quad (\text{B1-1})$$

“Peak” refers to the full energy peak in the gamma-ray spectrum that corresponds to the gamma-ray with energy  $E$ . According to Equation (B1-1), a peak intensity from a water-filled borehole measurement can be multiplied by  $K(E)$  to determine the intensity that would have been recorded if the water had been absent from the borehole.

Part of the SGLS base calibration involved logging the 4.5-inch, 7.0-inch, 9.0-inch, and 12.0-inch (diameter) test holes in the DOE-GJO KW Model, with and without water in the holes. The peak intensity data were used to derive the water corrections for Gamma 1A and Gamma 2A that are described in DOE (1995b).

The backup sonde was acquired about two years after the base calibration, and at that time the logging vehicles were in full time operation at Hanford and could not be transported to DOE-GJO to conduct the water correction measurements with Gamma 1B and Gamma 2B. Therefore, water-filled borehole log data recorded by Gamma 1B or Gamma 2B were corrected with the corrections for Gamma 1A or Gamma 2A. Although this followed normal oil industry practice, under which logging companies commonly determine corrections for a specific sonde, then apply those corrections to all sondes of identical or similar design, the MACTEC-ERS technical staff members decided to obtain data to justify this application. At the sixth recalibration (DOE 1999), new correction data were recorded by logging the Hanford calibration standard SBM with the four systems, first with liquid evacuated from the test hole, then with water in the test hole (SBM has only one test hole; the diameter is 4.5 inches). The primary reason was to show that the 4.5-inch-diameter water corrections for Gamma 1B and Gamma 2B were nearly identical to the corrections for Gamma 1A and Gamma 2A, respectively.

The sixth recalibration measurements confirmed that the 4.5-inch borehole corrections for Gamma 2A are essentially identical to the analogous corrections for Gamma 2B, and similarly, the corrections for Gamma 1A and Gamma 1B for the 4.5-inch borehole are nearly identical (DOE 1999). Also, for Gamma 2A the sixth recalibration corrections were nearly identical to the corrections from the base calibration. However, for Gamma 1A the sixth recalibration corrections were all significantly smaller than the base calibration corrections. Investigation confirmed a hypothesis stated in DOE (1995b), that

the correction data collected with Gamma 1A during the base calibration were unreliable because of electrical problems that afflicted the sonde when it was immersed in water. The spectral features that pointed to equipment problems, such as unusually large peak FWHM in the water-filled hole data, were not observed in the Gamma 1A sixth recalibration spectra, indicating that the problems were apparently corrected inadvertently during a service procedure aimed at a different problem. Though the Gamma 1A sonde is repaired, the water correction measurements for borehole diameters different from 4.5 inches cannot be repeated. Consequently, DOE (1999) recommends that the water corrections for Gamma 2A be used to process data collected with Gamma 1A, Gamma 1B, and Gamma 2B. The present discussion is therefore limited to corrections derived from the Gamma 2A data.

## B1.2 Gamma 2A Water Corrections

Data for the Gamma 2A corrections were gained by logging the KW Model at the base calibration (DOE 1995b), and the SBM standard at the first biannual recalibration (DOE 1996a). The KW Model logs yielded measurements for borehole diameters of 7.0 inches, 9.0 inches, and 12.0 inches, and the SBM logs yielded measurements for the 4.5-inch diameter. The KW Model and the SBM standard contain elevated concentrations of potassium, uranium, and thorium that provided gamma rays with many discrete energies.

Using Equation (B1-1), corrections were calculated for the numerous discrete gamma-ray energies and the four borehole diameters. Corrections were organized in sets, one set for each borehole diameter, and each set was analyzed with the *TableCurve* curve fitting program to determine an equation to use to calculate corrections for energies (e.g., 661.6 keV [ $^{137}\text{Cs}$ ]) that are not present in the calibration standards. The analyses indicated that  $K(E)$  for any of the four borehole diameters could be calculated for any observable energy  $E$  with

$$K(E) = \sqrt{A_w \% \frac{B_w}{E}}. \quad (\text{B1-2})$$

The uncertainty in  $K(E)$  is

$$s K(E) = \frac{1}{2K(E)} \sqrt{(s A_w)^2 \% \left( \frac{s B_w}{E} \right)^2}. \quad (\text{B1-3})$$

The factors  $A_w$  and  $B_w$  have constant values for a given borehole diameter. The values derived from the curve fitting analyses are displayed in Table B1-1.

*Table B1-1. Water Correction Constants for Four Borehole Diameters*

Borehole Diameter (inches)	$A_w$ (no units)	$B_w$ (kilo-electron-volts)
4.5	$1.2230 \pm 0.0024$	$128.7 \pm 1.4$
7.0	$1.733 \pm 0.014$	$1036 \pm 11$
9.0	$1.804 \pm 0.027$	$2654 \pm 22$
12.0	$-0.40 \pm 0.17$	$9082 \pm 153$

Equations (B1-2) and (B1-3) and the values of the water correction constants in Table B1-1, all of which are documented in DOE (1995b) and DOE (1996a), would have provided all that was needed for water corrections if the field boreholes had diameters matching the four diameters for which corrections were developed. However, the most common field borehole diameter (inner casing diameter) at Hanford turned out to be 6.0 inches. A few 4.0-inch-, 8.0-inch-, and 10.0-inch-diameter boreholes are also present.

Attempts to obtain values for  $A_w$  and  $B_w$  appropriate for the Hanford borehole diameters by curve fitting with borehole diameter as a variable produced accurate results but large uncertainties. As with the casing corrections, linear interpolation, rather than curve-fitting, yielded accurate  $A_w$  and  $B_w$  values with reasonable uncertainties.

### **B1.3 Reformulated Water Corrections**

The recommended method of deriving  $A_w$  and  $B_w$  values for the Hanford borehole diameters is linear interpolation over the diameter variable.

Symbols with white centers in Figures B1-1 and B1-2 show the experimental values of the water correction parameters  $A_w$  and  $B_w$  plotted in relation to borehole diameter.

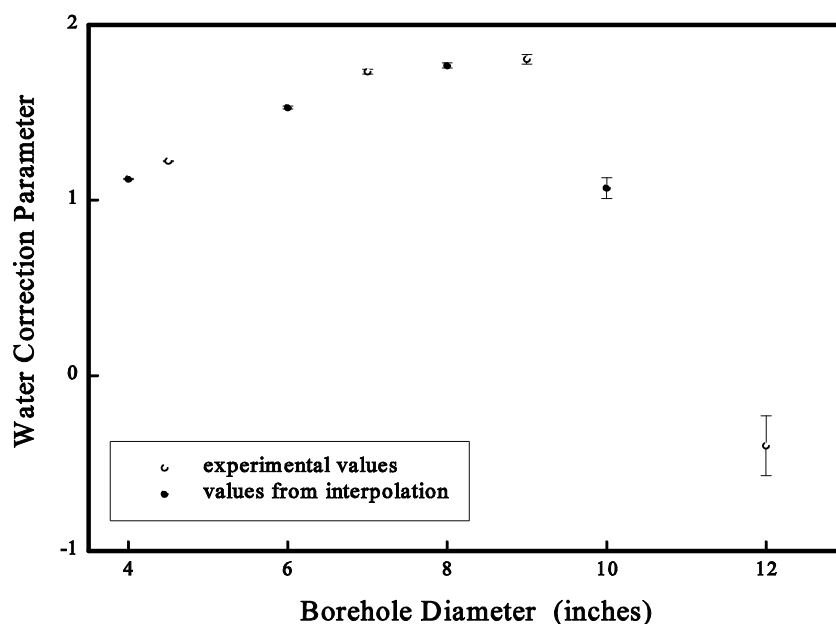


Figure B1-1. Parameter  $A_w$  Plotted as a Function of Borehole Diameter

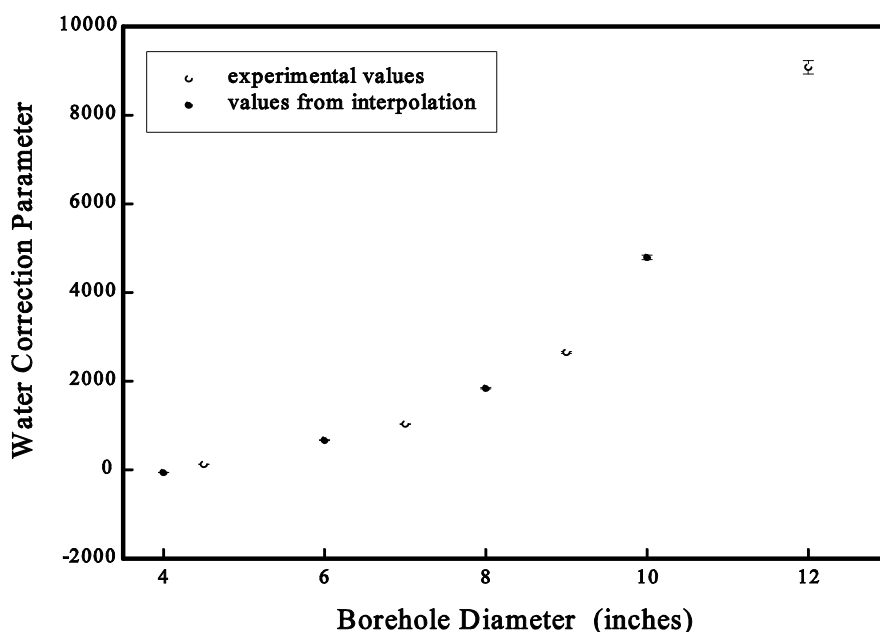


Figure B1-2. Parameter  $B_w$  Plotted as a Function of Borehole Diameter

The plotted symbols indicate that  $A_w$  and  $B_w$  are approximately linear in relation to borehole diameter between any two sequential data points, and thus linear interpolation could be applied to calculate values for  $A_w$  and  $B_w$  for any diameter between two diameters for which  $A_w$  and  $B_w$  were determined from measurements. In particular, if values for  $A_w$  and  $B_w$  were known for two particular diameters  $D_1$

and  $D_2$ , then the values for  $A_w$  and  $B_w$  for an intermediate diameter  $D$  ( $D_1 < D < D_2$ ) could be calculated as follows.

If  $A_1$  and  $A_2$  are the  $A_w$  values for the diameters  $D_1$  and  $D_2$ , respectively, and if  $B_1$  and  $B_2$  are the  $B_w$  values for the same diameters, then linear interpolation indicates that  $A_w$  and  $B_w$  for the intermediate diameter  $D$  ( $D_1 < D < D_2$ ) are

$$A_w = \left( 1 - \frac{D - D_1}{D_2 - D_1} \right) A_1 + \left( \frac{D - D_1}{D_2 - D_1} \right) A_2 \quad (\text{B1-4})$$

and

$$B_w = \left( 1 - \frac{D - D_1}{D_2 - D_1} \right) B_1 + \left( \frac{D - D_1}{D_2 - D_1} \right) B_2. \quad (\text{B1-5})$$

The associated uncertainties are

$$sA_w = \sqrt{\left( 1 - \frac{D - D_1}{D_2 - D_1} \right)^2 (sA_1)^2 + \left( \frac{D - D_1}{D_2 - D_1} \right)^2 (sA_2)^2} \quad (\text{B1-6})$$

and

$$sB_w = \sqrt{\left( 1 - \frac{D - D_1}{D_2 - D_1} \right)^2 (sB_1)^2 + \left( \frac{D - D_1}{D_2 - D_1} \right)^2 (sB_2)^2}. \quad (\text{B1-7})$$

Using the entries in Table B1-1 and Equations (B1-4) through (B1-7),  $A_w$  and  $B_w$  values and the associated uncertainties were calculated for the 6.0-inch, 8.0-inch, and 10.0-inch borehole diameters. The results are displayed in Table B1-2. Also displayed in the table are  $A_w$  and  $B_w$  values for the 4.0-inch borehole. The 4.0-inch borehole values were calculated with Equations (B1-4) through (B1-7), but because this borehole diameter is less than the smallest diameter for which measurements were conducted, the method utilized was actually linear extrapolation, not linear interpolation.

*Table B1-2. Water Correction Parameter Values for the Most Common Borehole Diameters at Hanford*

Borehole Inner Diameter (inches)	$A_w$	$B_w$
4.0	$1.1210 \pm 0.0040$	$-52.8 \pm 2.8$
6.0	$1.5290 \pm 0.0085$	$673.1 \pm 6.6$
8.0	$1.768 \pm 0.015$	$1845 \pm 12$
10.0	$1.069 \pm 0.060$	$4797 \pm 53$



The  $A_w$  and  $B_w$  values in Table B1-2 are depicted by black-centered symbols in the plots in Figures B1-1 and B1-2.

## B1.4 Summary

Using data from direct measurements, corrections for water-filled boreholes were calculated with Equation (B1-1) for many discrete gamma-ray energies and for borehole diameters of 4.5 inches, 7.0 inches, 9.0 inches, and 12.0 inches. Curve fitting with  $E$  as a variable indicated that the corrections as functions of the gamma-ray energy were well simulated by Equation (B1-2). The two parameters  $A_w$  and  $B_w$  in Equation (B1-2) assumed values that depended on the borehole diameter, as indicated in Table B1-1.

None of the field borehole diameters (4.0, 6.0, 8.0, and 10.0 inches) coincide with any of the diameters of the test holes in the calibration standards. However, values for the two correction parameters  $A_w$  and  $B_w$  in Equation (B1-2) were calculated by linear interpolation (with diameter as a variable) for the 6.0-inch, 8.0-inch, and 10.0-inch boreholes, and the  $A_w$  and  $B_w$  values for the 4.0-inch borehole were calculated by linear extrapolation.

The interpolation and extrapolation calculations yielded the  $A_w$  and  $B_w$  values listed in Table B1-2 and depicted by black-centered symbols in Figures B1-1 and B1-2. These values can be used with Equations (B1-2) and (B1-3) to calculate water corrections and correction uncertainties for the four field borehole diameters.

All of the water correction measurements were made with the sonde centered in the test holes. It follows that corrections calculated by methods described in this report are valid for log data acquired by centralized measurements. The corrections should not be used with data taken by eccentric measurements.

Another important point is that the data for the water corrections were collected with and without water in the test holes, and *no correction measurements were made with water and casing simultaneously present in the test holes*. The logging situation is different because all of the Hanford boreholes are cased, so if water occupies the borehole, gamma attenuation occurs in the casing, then in the water. It might seem straightforward and proper to apply both corrections to any particular spectral peak by multiplying the peak intensity by the casing correction, then multiplying the result by the water correction. However, this procedure will overcorrect the peak intensities, and the gamma source concentrations derived from the overcorrected intensities will be slightly but systematically higher than the true concentrations. The basis for this overcorrection lies in a subtle difference in radiation transport between the correction measurements and the field measurements. In the field borehole there is always casing between the formation and the water in the borehole. The (unscattered) gamma-ray flux impinging on the outer layer of casing from the formation is nearly isotropic, but the flux inside the casing is not isotropic, for the following reason. The gamma-ray path length inside the casing is  $T/\cos(\theta)$ , where  $T$  is the casing thickness,  $\theta$  is the azimuthal angle (measured relative to horizontal) and path length variations due to changes in polar angle are assumed negligible. That is, the smallest path lengths inside the casing are associated with small  $\theta$ , and because the least attenuation within the casing occurs

along the smallest path lengths, the gamma rays that pass through the casing are collimated to some degree around small azimuthal angles. Thus, the gamma rays that reach the water inside the casing are partially collimated along the direction corresponding to small  $\theta$ , which also corresponds to the smallest path lengths in the water. Consequently, the fraction of these gamma rays that pass through the water and reach the detector is greater than the fraction that would reach the detector if the flux passing from the casing to the water had been isotropic. Now, the water correction measurements were performed without casing in the test hole, so the gamma fluxes incident on the water from the formation were nearly isotropic and the attenuation of gamma rays in the water was relatively greater than would have been observed if the test hole had been cased. Thus, a smaller fraction of gamma rays reached the detector, relative to a cased hole measurement, and corrections calculated with Equation (B1-1), though valid for uncased boreholes, were consistently higher than the corrections that would have resulted if the dry and water filled borehole measurements had been done with casing in the test holes.

In summary, the application of the casing and water corrections to borehole data overcorrects the spectral peak intensities, and consequently, the calculated concentrations are systematically high. Problems associated with compound corrections were recognized in the early stages of the project, and in fact Section 8.1 in the base calibration report (DOE 1995b) notes that the correction for a thick casing is not identical to the combined corrections for two or more thin casings having a total thickness equal to the thickness of the thick casing. The reason is analogous to the casing and water situation; if the thick casing is regarded as equivalent to two collinear thin casings, then the correction for the thick casing would be slightly smaller than the combined corrections for the two thin casings because the correction for the inner thin casing would not have accounted for the collimation of gamma rays imposed by the outer thin casing.

The casing and water correction problem could have been averted by replicating the field borehole conditions in the calibration standard test holes. However, this could not be done because none of the calibration standards have test holes with diameters that match the diameters of the field boreholes.

At present, the Gamma 2A data are the only available water correction data that span a range of borehole diameters. Thus, the water correction parameter values for the Hanford borehole diameters in Table B1-2 were all derived from data recorded by Gamma 2A. For now, corrections calculated with these values should be applied to data taken with all of the logging systems.

Evidence that the universal application of the Gamma 2A corrections will not lead to inaccurate concentrations is presented in Figures B1-3 and B1-4. The curve in Figure B1-3 represents the 4.5-inch borehole corrections calculated with Equation (B1-2) and the  $A_w$  and  $B_w$  values for Gamma 2A, and the circles depict corrections measured with Gamma 1A and Gamma 1B at the sixth recalibration.

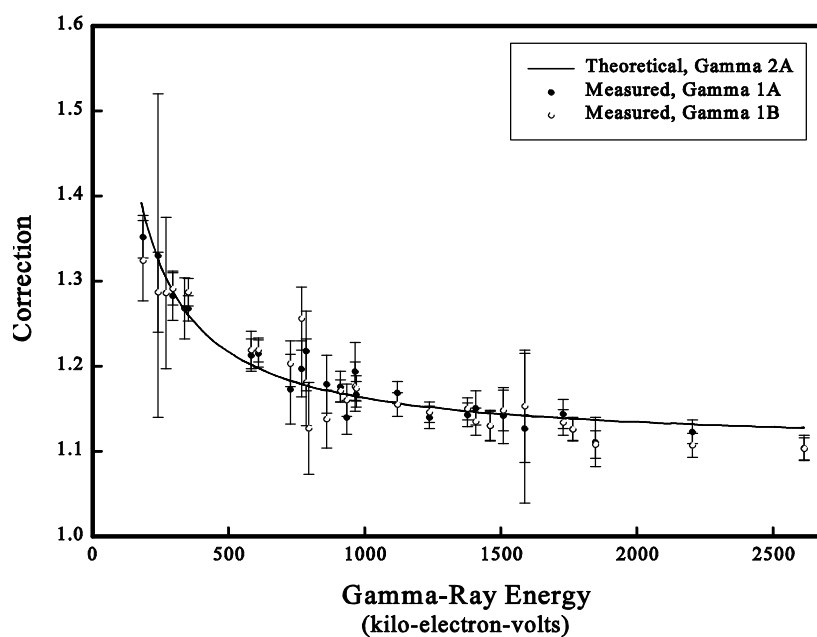


*Figure B1-3. Theoretical 4.5-inch Borehole Water Corrections for Gamma 2A Compared to Measured Corrections for Gamma 1A and Gamma 1B*

The curve in Figure B1-4 represents the 4.5-inch borehole corrections calculated with Equation (B1-2) and the  $A_w$  and  $B_w$  values for Gamma 2A, and the circles depict corrections measured with Gamma 2A and Gamma 2B at the sixth recalibration.

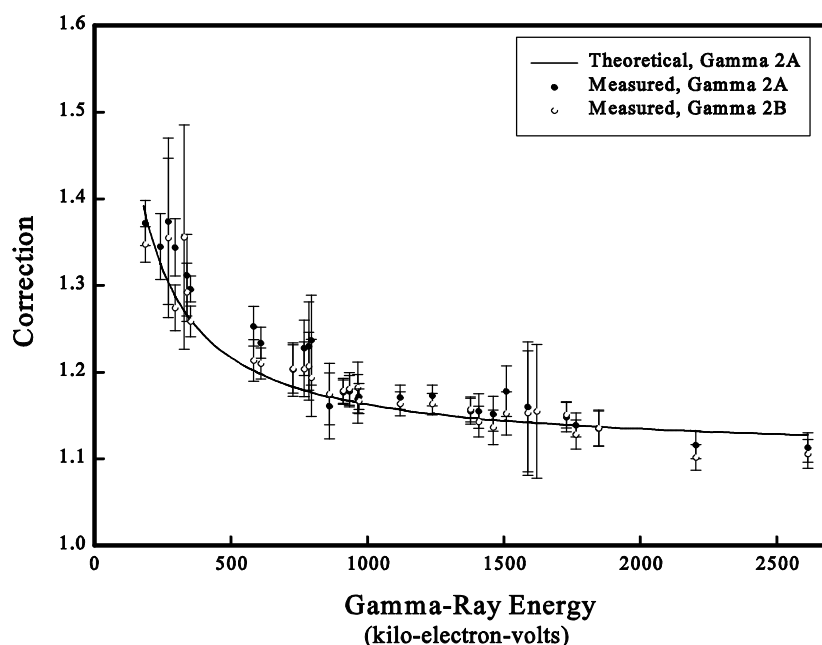


*Figure B1-4. Theoretical 4.5-inch Borehole Water Corrections for Gamma 2A Compared to Measured Corrections for Gamma 2A and Gamma 2B*

The graphs in Figures B1-3 and B1-4 support the contention that corrections calculated with Equation (B1-2) and the  $A_w$  and  $B_w$  values for Gamma 2A can be applied to data recorded with Gamma 1A, Gamma 1B, and Gamma 2B without corrupting the accuracies of the concentrations calculated from the corrected data.

For the 4.5-inch borehole, the corrections inferred from the base calibration data for Gamma 2A are nearly equal to the corrections derived from the sixth recalibration data for Gamma 2A, Gamma 2B, Gamma 1A, and Gamma 1B (DOE 1999). In contrast, the corrections derived from the base calibration data for Gamma 1A are about 20 percent higher than these corrections. DOE (1999) attributed the offset in the Gamma 1A corrections to unidentified electrical problems that affected the water-filled hole measurements at the base calibration. The graphs in Figure B1-3 show that the sixth recalibration measurements produced Gamma 1A corrections that essentially coincide with the Gamma 1B corrections. This indicates that the electrical problems that afflicted the Gamma 1A correction measurements at the base calibration have been corrected.